# Single-cell Transcriptome Mapping Identifies Common and Cell-type Specific Genes Affected by Acute Delta9-tetrahydrocannabinol in Humans

Ying Hu[1], Mohini Ranganathan [2,3], Chang Shu [2,3], Xiaoyu Liang [2,3], Suhas Ganesh [2,3], Chunhua Yan [1], Xinyu Zhang [2,3], Bradley E Aouizerat [4,5], John H Krystal [2,3], Deepak C. D'Souza[2,3], Ke Xu [2,3]

1. Center for Biomedical Information and Information Technology, National Cancer Institute, MD, U.S.A.

2. Department of Psychiatry, Yale School of Medicine, New Haven, CT, 06516

3. Connecticut Veteran Healthcare System, West Haven, CT, 06515

4. Bluestone Center for Clinical Research, College of Dentistry, New York University, NY, 10010

5. Department of Oral and Maxillofacial Surgery, College of Dentistry, New York University, NY, 10010

Please direct all correspondence to:

Ke Xu, MD, PhD

Associate Professor of Psychiatry

Yale School of Medicine

Email: ke.xu@yale.edu

Telephone: 203-932-5711x7430

**Abstract**

Delta 9-tetrahydrocannabinol (THC), the principal psychoactive constituent of cannabis, is also known to modulate immune response in peripheral cells. The mechanisms of THC's effects on gene expression in human immune cells remains poorly understood. Combining a within-subject design with single cell transcriptome mapping, we report that administration of THC acutely alters gene expression in 15,973 human blood immune cells. Controlled for high inter-individual transcriptomic variability, we identified 294 transcriptome-wide significant genes among eight cell types including 69 common genes and 225 cell-type specific genes affected by acute THC administration, including those genes involving not only in immune response, cytokine production, but signal transduction, and cell proliferation and apoptosis. We revealed distinct transcriptomic sub-clusters affected by THC in major immune cell types where THC perturbed cell type-specific intracellular gene expression correlations. Gene set enrichment analysis further supports the findings of THC's common and cell-type specific effects on immune response and cell toxicity. We found that THC alters the correlation of cannabinoid receptor gene, *CNR2,* with other genes in B cells, in which *CNR2* showed the highest level of expression. This comprehensive cell-specific transcriptomic profiling identified novel genes regulated by THC and provides important insights into THC's acute effects on immune function that may have important medical implications.

**Key words**: Delta-9-tetrahydrocannabinol, single cell transcriptome, peripheral blood mononuclear cells, differential gene expression, gene set enrichment analysis, gene co-expression

## Main

With the increasing rates of cannabis use for recreational and medical purposes, it is important to address a gap in our understanding of its impact on immune and inflammatory functions.[1,2] Delta-9-tetrahydrocannabinol (THC), the principal psychoactive constituent of cannabis, powerfully modulates immune function in peripheral cells,[3] in part, through activating cannabinoid receptor 2 (CBR2).[1,3-6] *In vitro* studies of cannabis exposure, which contains over 450 compounds, show that it modulates immune function,[7-9] changes cytokine production,[8,10,11] inhibits cell proliferation,[2] and induces apoptosis.[12,13] However, little is known about the mechanisms of *in vivo* THC exposure on the transcriptomes of distinct types of peripheral blood mononuclear cells (PBMCs) in humans.

Single cell RNA-seq (scRNA-seq) offers an unprecedented resolution to detect drug effects on cell-specific gene expression in an unbiased fashion[14,15] and enables the evaluation of molecular aspects of immune cell heterogeneity.[16] Few studies have applied scRNA-seq to detect differentially expressed genes (DEGs) induced by drug exposure, and none have evaluated the effects of THC in humans. This limitation is due mostly to high inter-individual transcriptomic variability and types of cells that confound the assessment of the impact of environmental factors. Most recently, a scRNA-seq study identified a large number of common and cell-type specific DEGs for Alzheimer disease, suggesting the improvement of analytical methods to overcome the challenge of high transcriptomic variability.[17] Here, we report a first sc-RNA seq study using within-subject combined with linear mixed model (LMM) analysis to detect genes affected by THC at single cell resolution.

In this study, samples of blood were drawn and PMBCs extracted prior to (pre-THC) and 70 minutes following (post-THC) a single 0.03mg/kg intravenous dose of THC in two healthy individuals. The selected THC dose reliably produces effects consistent with cannabis intoxication.[18,19] The timing of the blood sampling was selected to maximize the likelihood of

detecting changes in drug-induced gene expression. A battery of subjective and cognitive assessments were administered to capture the effects and safety of THC.[18,20,21] We profiled the four PBMC samples (two pre-THC and two post-THC) on the 10X Genomics platform.[22] Quality control processing yielded a total of 15,973 cells and 21,430 genes for analyses (**Figure 1a**).

Cells (n=15,973) clustered by participant, not by experimental condition (**Figure 1b**), indicating that transcriptomic variability between individuals is greater than variability introduced by a single THC dose. We then removed batch effects using Seurat [23] and surrogate variable analysis [24] methods and all 15,973 cells clustered into 21 groups (**Figure 1c, Figure S1**). To assign cell clusters to cell types, we used a generalized linear model (GLM)-based cell mapping approach with cell-type "marker" genes curated from the literature (see Methods). Briefly, we selected a reference gene panel based on known cell type-specific gene profiles [22,25], then used GLM to test the association of gene expression in each cell with the known marker genes(Figure S2, Table S1) . Each cluster was assigned a cell type based on the highest percentage of significant cells (**Table S2**). Expression of marker genes differed significantly in cell types (**Figures 1d**, **S2**). This approach unambiguously deconvoluted the 15,973 cells among 21 clusters into eight cell subtypes: CD4+ T-cells (34.6%), IL7RCD4+ T-cells (8.4%), CD8+ T-cells (17.4%), B cells (13.2%), natural killer (NK) cells (12.3%), CD14+ monocytes (10.0%), FCGR3A monocytes (3.9%), and dendritic cells (DC) (0.3%) (**Figure 1e**). The proportions of each cell type among the participant samples pre- and post-THC infusion are presented in **Figure 1f** and **Table S3**. This robust cell type identification allowed us to examine THC-regulated gene expression in each cell type.

We next applied LMM to detect individual genes affected by THC infusion, with participant included as a random variable to limit confounding effects from an individual's genomic background. We identified 294 transcriptome-wide significant genes in eight cell types changed by THC infusion (false discovery rate, FDR<0.05) (**Figure 2a**). DCs and FCGR3A monocytes

were excluded from further analyses because no gene reached transcriptome-wide significance in DCs and both cell types had low frequencies. Among the 294 DEGs, 69 were observed in at least two cell types while 225 were significant in unique cell types (**Figure 2b**; **Table S4-S11**). Overall, THC infusion resulted in more upregulated genes than downregulated genes.

We sought to identify THC-regulated genes common across the six common cell types. We found 28 DEG in at least three cell types (**Figure 2c**). The majority of the DEG showed consistent directions of regulation by THC in different cell types; only three genes displayed opposing regulation in CD14+ monocytes compared to other cell types (*TMSB4X*, *JUNB, TXNIP*). A group of THC-regulated genes have functions in the domains of immune response and inflammatory process. For example, expression of *S100A9* and *S100A8*, which play prominent roles in the regulation of proinflammatory processes and immune response[26-28], decreased in response to THC infusion in five cell types. A major HIV-1 suppressive gene, *CCL4,* displayed increased expression after THC infusion. THC decreased expression of *GNLY* that is involved in activating antigen presentation.[29] The altered expression of genes involved in humoral immunity were also observed (*IGLC2, IGKC)*. Changes in expression of these genes suggest that THC activates the adaptive immune system shortly after administration, in a line with findings showing an immunomodulatory effect that is more complicated than solely immunosuppression.[3,8,30-33]

Among the 28 DEG shared in at least three cell types, a subset supports previous findings that acute THC exposure inhibits cell proliferation and induces apoptosis. Genes responsible for cell death were upregulated (*BTG1,*[34] *DDIT4,*[35] *GZMB*) and genes involving in cell growth and differentiation were down-regulated (*TMSB10*[36], *RPS21*,[37] *RPL41*[38] by THC exposure. The alteration of these genes in distinct cell types may indicate potentially deleterious effects of THC on cell differentiation and survival.

Given that the majority of THC-regulated DEG are unique to each cell type, we then focused on DEG and co-expression networks in each cell type. DEG were determined both in individual clusters in each cell type and among all cells in each cell type. We leveraged gene-gene relationships cataloged in the Kyoto Encyclopedia of Genes and Genomes (KEGG) database[39] and constructed gene networks independently in pre- and post-THC samples in each cell type (FDR<0.05). Hub genes in each cell-type based network were defined as a node (gene) with at least four edges (gene links) in at least one condition (pre-, post-THC, or both). We then performed Gene Ontology (GO) term enrichment analysis for each cell-type based co-expression network (FDR<0.05).

In CD4+ T-cells, significant DEG are involved in cytotoxic T-cell activation (*IL7R*[40]), histone modification (*H3F3B*[41]), and transcriptional regulation (*MYC*[42]). We observed three cell sub-groups (cluster 3, 8, and 16; **Figure 3a**; **Table S12**). Cluster 8 showed a distinct DEG pattern from clusters 3 and 16. Co-expression analysis identified 40 nodes with 33 edges enriched on 14 GO terms including immune response, cell surface receptor signaling pathway, cellular response to stimulus. Two hub genes in the network, *CCR7* (significantly connected with *CCR* [*CCR2, CCR6, CCR10*] and *CXCR* [*CXCR3*, *CXCR4*] family genes) and *HLA-A* (significantly correlated with three other *HLA* genes [*HLA-B, HLA-E, HLA-F*], were significantly affected by THC infusion (**Figure 3b**), showing that acute THC exposure perturbed gene-gene relationships in CD4+ T-cells and appears to increase the gene connectivity involving cell-mediated immunity.

In CD8+ T-cells, we identified 18 unique DEGs that involved in immune response and inflammation in response to THC (e.g. *IL32*,[43] *SOCS1*,[44] and *IRF1*[45]) . Of note, THC infusion resulted in the differential expression of *CXCR4, TSC22D3, DDIT4, BTG1, JUN* in cluster 18 of CD8+ T-cells (**Figure 3c**), suggesting that cells in cluster 18 may function differently in response to THC as compared to the other CD8+ T-cell sub-group. The gene network included 35 nodes that enriched on 12 GO terms (e.g., immune system process), similar to the CD4+ T-cell

network. One hub gene, *HLA-A* (strongly correlated with *HLA-B* and *HLA-C* in pre-and post-THC samples), was observed in the network (**Figure 3d**; **Table S13**).

In B cells, genes unique to B cells were observed that are involved in B cell maturation (*VPREB3*[46]), MHC function (*HLA-DQA1*, *HLA-DQA2*), calcium signaling (*CALM2*),[47] Toll-like receptors (*CD180*),[48] and response to environmental stress via activating MAP kinase MAPK1/ERK2 (*DUSP1*).[49] Consistent with *in vitro* findings, we found that acute THC exposure reduced expression of *BCL2* in B cells.[40] The majority of DEG originated from cluster 14 (**Figure 3e**; **Table S14**), with only 8 DEGs from cluster 12, which were all upregulated by THC. In the co-expression network, we found 34 nodes with 28 edges (**Figure 3f**) enriched on GO pathways including MHC protein complex, immune response, peptide antigen binding. Four hub genes were identified that differed in response to THC (*HLA-A and HLA-BQA1) HLA-DPA1* [became more strongly correlated with *HLA-DQB1* post-THC]*, ANX1* [connected to *CXCL1*, *CXCR4*, *XOL2* in pre-but not post-THC samples]). Notably, two B cell marker genes (*BLNK*, *CD79B*) were correlated in post- but not pre-THC samples.

In NK cells, which is defined by one cluster, many DEGs (e.g. *DDIT4, CCL4, BTG1 ID2*) are involved in immune response and cell proliferation. One DEG unique to NK cells, *CD53*, was downregulated by THC. Genes in the NK cell network (17 nodes and 12 edges; **Figure 3g**) were enriched on 17 pathways including chemokine-mediated signaling pathway, inflammatory response, and chemokine receptor activity. Notably, *KLRC1* regulates specific humoral and cell-mediated immunity and is implicated in the recognition of the MHC class I HLA molecules in NK cells and was correlated with *HLA-C*, which increased in post-THC samples. No hub genes were observed.

In CD14+ monocytes, which were composed of two subgroups (cluster 10 and 17; **Figure 3h**; **Table S15**), THC infusion resulted in unique 44 DEGs, including genes regulating cell fate (e.g. *MCL1*, *FOSB*, *MYADM*). Genes in the CD14+ monocyte network (18 nodes and 13 edges;

**Figure 3i**) were enriched on pathways including MHC class II protein complex, antigen processing, immune response, and cellular response to interferon-gamma. One hub gene, *HLA-DQB1*, was observed.

These observations from individual gene and co-expression networks in different cell types suggest a diverse functional response to acute THC exposure in heterogenous immune cells. Significant pathways for all co-expression networks in each major cell type are presented in Table **S16-S21**.

We subsequently performed a cell type-based gene set enrichment analysis (GSEA) using DEGs. We found 39 significant KEGG pathways in at least two cell types (**Figure 3j**; **Table S22-S29**); significant pathways were involved in the domains of immune response, inflammation, and cell survival and apoptosis. Several pathways associated with autoimmune disease (e.g., rheumatoid arthritis) were significant in multiple cell types. The ribosomal pathway, which plays a role cell growth and cellular response to stress, was the most significantly enriched pathway across all five cell types. These results further support the effects of THC on functional domains in immune regulation that have also been associated with immunological disease, although the causality of these relationships is unknown.

Finally, we were interested in understanding how cannabinoid receptor genes co-expressed with other genes in each cell type following THC administration. As expected, *CNR2*, encoding for CBR2, was highly expressed in B cells, followed by NK cells, then CD8+ T-cells, and lowest in CD4+ T-cells (**Figure 4a**).[50] Little *CNR1* expression was detected in any of the cell types. *GPR55* (cannabinoid receptor 3[51]) showed the highest expression in CD4+ T-cells. We observed gene co-expression between *CNR2* and 84 and 74 genes in pre- and post-THC samples, respectively (**Table S30-S31**). The co-expressed genes in post-THC B cells were enriched on functional domains of immune processes, biological regulation, cell proliferation, signaling, and response to stimulus (**Figure 4b**).

In summary, our results from a well-controlled, within subject human study demonstrate transcriptomic regulation in distinct immune cells following administration of a single dose of THC. Our study design and analytical approach enabled the identification of common and cell-type specific DEGs regulated by THC. Subjective, behavioral and cognitive tests confirm that the dose of THC was relevant to but limited the confounding effects of other compounds in cannabis. The cell type-specific gene and co-expression patterns revealed by scRNA-seq showed little overlap across cell types, which would have been obscured by bulk RNA-seq analysis. Cell type-based DEGs, co-expression networks, and GSEA revealed important THC effects on immune function, cytokine production, signal transduction, and cell apoptosis and survival. The study provides a foundation for future studies of cell type-specific immunologic effects of cannabis and cannabinoid constituents. Studying the effects of chronic medicinal or recreational cannabinoid exposure or the effects in immune disorders (e.g., HIV) using our approach are also warranted. These findings highlight the complexity of cannabinoid effects on immune function and nuance of immune cell types that may have medical relevance.

## Methods

The study was conducted at the Neurobiological Studies Unit (VA Connecticut Healthcare System, West Haven, CT) with the approval of the Institutional Review Boards at VA Connecticut and Yale University, and the Protocol Review Committee of the Department of Psychiatry, Yale University. The study was amended to include prospective measures addressing safety.

### *Participants*

Two healthy participants were recruited from the community by advertisements. Both participants were male, 21-year old, and of European American descent. Subjects were

informed about the potential for psychosis, anxiety, and panic. After obtaining informed consent, subjects underwent a structured psychiatric interview for DSM-IIIR [52] and were carefully screened for any DSM-IV Axis I or Axis II lifetime psychiatric or substance abuse disorder (excluding nicotine) and family history of major Axis I disorder. The history provided by subjects was confirmed by a telephone interview conducted with an individual (spouse or family member) identified by the subject prior to screening. In order to avoid exposing cannabis-naïve individuals to a potentially addictive substance, only subjects who had been exposed to cannabis but did not meet lifetime criteria for a cannabis use disorder were included. Past month cannabis use was quantified using a time-line-follow-back approach. Finally, subjects underwent a general physical and neurologic examination, EKG, and laboratory tests (serum electrolytes, liver function tests, complete blood count with differential and urine toxicology). Subjects were instructed to refrain from caffeinated beverages, alcohol, and illicit drugs from 2 weeks prior to testing until study completion. Urine toxicology was conducted on the morning of each test day to rule out recent illicit drug use.

***Procedure***

Subjects received 0.03mg/kg of THC, the principal active ingredient of cannabis.[18,19] This dose equivalent to 2.1 mg in a 70 kg individual has been shown in previous studies to produce effects consistent with the known effects of cannabis, in a safe manner.[53-55] THC was administered on its own, without the >450 other chemical constituents of cannabis because THC is the principal active constituent of cannabis and the other chemical constituents could render the results challenging to interpret. The intravenous route of administration was chosen to reduce inter and intraindividual variability in plasma THC levels with the inhaled route.[56] Timeline of behavioral assessment and blood draw is presented in **Figure S3**. Subjects were attended to by a research psychiatrist, a research nurse, and a research coordinator. Clear 'stopping rules' were determined a priori and rescue medication (lorazepam) was available if necessary. Medical

246 condition and psychiatric status of participants were monitored closely during and after THC
247 challenging. Subjective and clinical ratings were repeatedly assessed.

248 ***Medical and behavioral assessment***

249 Vital signs, Cannabis intoxication, Psychotic symptoms, Perceptual alteration, and Cognitive
250 test battery were measured prior, during, and post THC infusion as illustrated in **Figure S3**.

251 ***Single cell RNA sequencing in 10X Genomics platform***

252 PBMCs from pre-THC (N=2) and post-THC samples (N=2) from fresh whole blood were isolated
253 at the same time using a standard protocol. The cells were washed twice with phosphate-
254 buffered saline containing 0.04% bovine serum albumin, and the final cell concentration was
255 adjusted to 1000 cells/mL for library preparation. 5000 cells/sample were prepared for single
256 cell capture.

257 *Sequencing data processing and quality control*

258 We used the 10X Genomics Chromium Single Cell 3' v2.0 platform to prepare individually
259 barcoded single-cell RNA-Seq libraries following the manufacturer's protocol. Library size was
260 confirmed with Agilent Bioanalyzer High Sensitivity DNA assay (PN:5067-4626), Invitrogen
261 dsDNA HS qubit assay to evaluate dsDNA quantity (PN: Q32854), and KAPA qPCR analysis
262 (KAPA Biosystems LIB Quant Kit, Illumina/LC480, PN: KK4854) to evaluate the quantity of
263 sequencable transcripts.

264 *Flow Cell Preparation and Sequencing*: Sample concentrations are normalized to 10 nM and
265 loaded onto Illumina Rapid flow cell at a concentration that yields 150M passing filter clusters
266 per lane. Samples are sequenced using paired-end sequencing on an Illumina HiSeq 2500
267 according to Illumina protocols. The 8 bp index is read during an additional sequencing read

that automatically follows the completion of read 1. Data generated during sequencing runs are simultaneously transferred to the YCGA high-performance computing cluster. A positive control (prepared bacteriophage Phi X library) provided by Illumina is spiked into every lane at a concentration of 0.3% to monitor sequencing quality in real time.

*Data Analysis and Storage*: Signal intensities are converted to individual base calls during a run using the system's Real Time Analysis (RTA) software. Base calls are transferred from the machine's dedicated personal computer to the Yale High Performance Computing cluster via a 1 Gigabit network mount for downstream analysis. Primary analysis - sample de-multiplexing and alignment to the human genome - is performed using Illumina's CASAVA 1.8.2 software suite. The Cell Ranger Single-Cell Software Suite (versions 2.0.0 and 2.1.0 for the discovery and validation patients respectively) were used to perform sample demultiplexing, barcode processing and single-cell gene counting (http://10xgenomics.com/). The gene-cell matrix was generated for the following analysis.

*Data normalization*

Only genes with at least one UMI count detected in at least one cell were retained for analysis Single cells were excluded when >10% of reads mapped to mitochondrial RNA to ensure that all of the single cells originated from nucleated cells. The cells with fewer than 370 expressed genes or possible doublet cells (>100,000 reads) were also discarded. Applying these three criteria resulted in retention of 21,430 genes and 15,973 single cells for downstream analysis.

Data normalization was performed using a standard protocol in Seurat.[23] An exploratory analysis showed cells clustered by each participant. Batch effects were then removed using an empirical Bayesian framework (ComBat function in R package sva) with the individual labeled as the random variable. The normalized data was dimensionally reduced in two dimensions using t-distributed stochastic neighbor embedding (t-SNE) with a perplexity parameter of 20 and

3000 iterations after an initial principle component analysis. The distance matrix of the single cells was computed with the output of tSNE and converted into a graph. Then, the graph was clustered with the cluster_louvain function in R package *igraph*, which implements the multi-level optimization of modularity algorithm for finding community structure.

*Cell type identification*

A gene set of the cell type markers in PBMC was manually curated from the literature. A binary cell type matrix with cell types as columns and genes as rows was generated with value 1 representing a marker in a cell type and value 0 denoting non-markers for a cell type. The generalized linear model (GLM) was constructed by deciding on one vector, representing one cell type as response, of the binary matrix and corresponding gene expressions as explanatory variables in one cell. In details, $\boldsymbol{Y} = \left(y_{gc}\right)_{G\times C}$ is the binary cell type matrix of $G$ marker genes of $C$ cell types and $\boldsymbol{X} = \left(x_{gs}\right)_{G\times S}$ is the gene expression matrix of $G$ marker genes of $S$ single cells. For the $g^{th}$ gene, $y_{gc} = 0$ or $1$ denotes the cell type-specific gene indicator of $c^{th}$ cell type and $x_{gs}$ denotes the gene expression of $s^{th}$ single cell, where $g = 1, \dots, G$, $c = 1, \dots, C$, and $s = 1, \dots, S$. The linear probability model (LPM) was conducted for our study, $\boldsymbol{y_c} = \beta_{0cs} + \beta_{1cs}\boldsymbol{x_s} + \boldsymbol{\varepsilon_{cs}}$, where $\boldsymbol{y_c} = (y_{1c}, \dots, y_{Gc})^T$ and $\boldsymbol{x_s} = (x_{1s}, \dots, x_{Gs})^T$ are the columns of matrix $\boldsymbol{Y}$ and $\boldsymbol{X}$, represent binary cell type vector and single cell gene expression vector, respectively. $\boldsymbol{\varepsilon_{cs}} = (\varepsilon_{1cs}, \dots, \varepsilon_{Gcs})^T$ is a random error vector, where $\varepsilon_{gcs} \sim N(0, \sigma^2)$. The hypothesis of interest to be tested is $H_{0cs}: \beta_{1cs} = 0$ vs $H_{1cs}: \beta_{1cs} \neq 0$. One statistical value (t value) and p value is obtained for each cell and cell type; $t_{cs}$ and $p_{cs}$ denote the test statistic value and P-value, respectively for the $c^{th}$ cell type of $s^{th}$ single cell.

We used the cutoff, p < $p_0$ and t value > 0 to assign one cell to one cell type, where $p_0$ is a predefined cut-off value ($p_0 = 0.01$ in this study). Then, the proportion of each assigned cell type

was calculated for every cluster. The dominant proportions are used to assign one cluster to one cell type.

$$P_c^k = \frac{\sum_{s \in S_k} \left( I(t_{cs} > 0) \cdot I(p_{cs} < p_0) \right)}{N_k},$$

where $P_c^k$ denotes the proportion of the $c^{th}$ cell type in the $k^{th}$ cluster. $S_k$ is the set of cell indices for clustering $k$, with $N_k = |S_k|$ being the total number of cells in the $k^{th}$ cluster. Finally, the cell type for each cluster was confirmed manually by cell type marker gene expressions mapping on the 2D tSNE plot. The cell clusters mapping to the same cell type were merged for downstream analysis.

***Statistics***

All statistical analyses were performed using R version 3.5.1 (R Foundation, https://www.r-project.org) and RStudio version 1.1.453 (https://www.rstudio.com).

*Differential gene expression.* We applied a linear mixed regression model to identify genes associated with THC infusion. To control transcriptomic variation between two participants, we used participant as a random effect. Transcriptome-wide significance was set at false discovery rate (FDR) <0.05.

*Cell type-based gene-gene correlation analysis*. The relationship among genes in each given cell type was from KEGG database. We tested whether gene links in KEGG were significant in each cell type using linear regression model. Significant gene-gene correlation was set at FDR<0.05. The analysis was performed separately in pre-THC and post-THC samples to test if THC alters gene-gene correlation.

*Gene Ontology (GO) enrichment analysis*. Genes in each co-expression network in major cell types were tested the enrichment on GO terms using The DAVID Gene Functional Classification Tool.[57] Significant level was set at FDR <0.05.

*Cell type-based gene set enrichment analysis*. We separately analyzed gene set enrichment in each cell type using KEGG database. Differentially expressed genes in a given cell type with nominal $p < 0.001$ were selected. Significant pathway was set at FDR <0.05.

*Co-expression of cannabinoid receptor genes with other genes*: Four cannabinoid receptor genes, *CNR1, CNR2, CPR18,* and *GPR55* were tested differential expression across seven major cell types using linear mixed regression model. Correlation of *CNR2* with other genes in B cells was performed in pre- and post-THC samples independently. Significant correlation was set at FDR <0.05.

**Reporting summary**

Further information about study design, codes, and statistics are in the reporting summery.

**Data availability**.

Single cell transcriptome data have been deposited in Gene Expression Omnibus and are available under project number GSE130228.

**Acknowledgement**

This work was supported by the National Institute on Drug Abuse grants R01DA047820 (PI: Xu), R01DA047063 (PI: Xu), R01042691 (PI: Xu), and 1R21AA024257 (PI: D'Souza). Suhas Ganesh is partially supported by a NARSAD Young Investigator grant from the Brain and Behavior Research Foundation.

The authors thank Wenzhong Liu, Child Study Center at Yale University, Jaime Heltke, Guilin Wang, Christopher Castaldi at Yale Center of Genomic Analysis for supports of single cell RNA

sequencing. The Veterans Affairs Connecticut Healthcare System (VACHS), West Haven. The nurses (Angelina Genovese, Elizabeth O'Donnell and Margaret Dion-Marovitz) of the Neurobiological studies Unit, and the research pharmacist (Rachel Galvan) of VACHS.

**Contributions**

K. Xu, Y. Hu, B. Aouizerat, D.C. D'Souza, J. H. Krystal designed the study and wrote the manuscript. Y. Hu, C. Shu, X. Liang, C. Yan, analyzed data. M. Ranganathan, S. Ganesh, and D.C. D'Souza were responsible for participant recruitment and THC infusion. All authors contributed to manuscript preparation.

**Competing interests**

All co-authors except Dr. Krystal declare no completing interests

The following competing interests for John H. Krystal:

**RE: John H. Krystal, MD**

**2019 Financial Disclosure**

Consultant

Note: – The Individual Consultant Agreements listed below are less than $10,000 per year

AstraZeneca Pharmaceuticals

Biogen, Idec, MA

Biomedisyn Corporation

Bionomics, Limited (Australia)

Boehringer Ingelheim International

Concert Pharmaceuticals, Inc.

Epiodyne, Inc.

Heptares Therapeutics, Limited (UK)

Janssen Research & Development

L.E.K. Consulting

Otsuka America Pharmaceutical, Inc.

Perception Neuroscience Holdings, Inc.

Spring Care, Inc.

Sunovion Pharmaceuticals, Inc.

Takeda Industries

Taisho Pharmaceutical Co., Ltd

Scientific Advisory Board

Bioasis Technologies, Inc.

Biohaven Pharmaceuticals

BioXcel Therapeutics, Inc. (Clinical Advisory Board)

Cadent Therapeutics (Clinical Advisory Board)

PsychoGenics, Inc.

Stanley Center for Psychiatric research at the Broad Institute of MIT and Harvard

Lohocla Research Corporation

Stock

ArRETT Neuroscience, Inc.

Biohaven Pharmaceuticals

Sage Pharmaceuticals

Spring Care, Inc.

Stock Options

Biohaven Pharmaceuticals Medical Sciences

BlackThorn Therapeutics, Inc.

Storm Biosciences, Inc.

Income Greater than $10,000

Editorial Board

Editor - Biological Psychiatry

Patents and Inventions

1) Seibyl JP, Krystal JH, Charney DS. Dopamine and noradrenergic reuptake inhibitors in treatment of schizophrenia. US Patent #:5,447,948.September 5, 1995

2) Vladimir, Coric, Krystal, John H, Sanacora, Gerard – Glutamate Modulating Agents in the Treatment of Mental Disorders US Patent No. 8,778,979 B2 Patent Issue Date: July 15, 2014. US Patent Application No. 15/695,164: Filing Date: 09/05/2017

3) Charney D, Krystal JH, Manji H, Matthew S, Zarate C., - Intranasal Administration of Ketamine to Treat Depression United States Application No. 14/197,767 filed on March 5, 2014; United States application or Patent Cooperation Treaty (PCT) International application No. 14/306,382 filed on June 17, 2014

4): Zarate, C, Charney, DS, Manji, HK, Mathew, Sanjay J, Krystal, JH, Department of Veterans Affairs “Methods for Treating Suicidal Ideation”, Patent Application No. 14/197.767 filed on March 5, 2014 by Yale University Office of Cooperative Research

5) Arias A, Petrakis I, Krystal JH. – Composition and methods to treat addiction.

Provisional Use Patent Application no.61/973/961. April 2, 2014. Filed by Yale University Office of Cooperative Research.

6): Chekroud, A., Gueorguieva, R., & Krystal, JH. “Treatment Selection for Major Depressive Disorder” [filing date 3rd June 2016, USPTO docket number Y0087.70116US00]. Provisional patent submission by Yale University

7) Gihyun, Yoon, Petrakis I, Krystal JH – Compounds, Compositions and Methods for Treating or Preventing Depression and Other Diseases. U. S. Provisional Patent Application No. 62/444,552, filed on January10, 2017 by Yale University Office of Cooperative Research OCR 7088 US01

8) Abdallah, C, Krystal, JH, Duman, R, Sanacora, G. Combination Therapy for Treating or Preventing Depression or Other Mood Diseases. U.S. Provisional Patent Application No.

047162-7177P1 (00754) filed on August 20, 2018 by Yale University Office of Cooperative Research OCR 7451 US01

NON-Federal Research Support

AstraZeneca Pharmaceuticals provides the drug, Saracatinib, for research related to NIAAA grant “Center for Translational Neuroscience of Alcoholism [CTNA-4]

## Figure Legends

**Figure 1 A flow chart illustrating the study design and data analysis strategy**.

a. Two participants were infused with delta-9-tetrahydrocannabinol (THC). Blood samples were drawn before and 70 minutes after THC infusion. Peripheral blood mononuclear cells (PBMC) were isolated from each sample and 5000 cells subjected to single cell RNA-seq using the 10X Genomics platform.

b. tSNE plot showing cell transcriptomic clusters of 15,973 PBMCs in four samples pre- and post-THC infusion: pre-THC-S1; 65: post-THC-S1; pre-THC-S2; and post-THC-S2. Cell number in each sample are presented. The plot indicates a batch effect by participants showing that cell clustered by two participants.

c. After removal of batch effects from two participants, 15,973 cells clustered into 21 groups by single cell transcriptomic profile.

d. Examples of differentially expressed marker genes in each cell cluster. The clusters with similar marker gene profiles in a given cell type were assigned to the same cell type: CD4+ T-cells Clu(2,3,8,13,15,16,19); IL7RCD4+ T-cells Clu(4); CD8+ T-cells Clu (1,7,18,20,21); B cells Clu(6,12,14); NK cells Clu(5) CD14+ monocytes Clu(10,17); FCGR3A monocytes Clu(9) DCs Clu(11).

e. Cell type identification by generalized linear modeling (GLM) cell mapping approach and tSNE plotting. A panel of reference genes for each cell type were selected from previously published studies. GLM tested the association of cell type and marker gene expression in each cell. Significance association is set at $p<0.02$ and $t>0$. Each individual cell is assigned to a cell type based on the predominant proportion of marker genes in a given cell type. Small cell clusters are merged into the closest cell type in the tSNE plot. The cell mapping deconvolutes

cells to eight PBM cell types: CD4+ T-cells, ILR7+/CD4+ T-cells, CD8+ T-cells, B cells, natural killer cells, CD14+ monocytes, FCGR3A monocytes, and DCs.

f. Percentage of cell numbers from each sample in a given cell type: pre-THC-S1, post-THC-S1, pre-THC-S2, post-THC-S2.

**Figure 2 Single cell transcriptome profiling reveal gene expression affected by a single dose of delta-9-tetrahydrocannabinol**

a. Linear Mixed Regression analysis identified differential expression of genes affected by THC infusion in eight cell types of peripheral blood mononuclear cells: CD4+ T-cells, ILR7CD4+ T-cells, CD8+ T-cells, B cells, natural killer cells, CD14+ monocytes, FCGR3A monocytes, and DCs. Differentially expressed genes were identified by applying linear mixed modelling (false discovery rate, FDR<0.05). Each inset box denotes the number of up-regulated (right box) and down-regulated (left box) genes. No differentially expressed genes were found in DCs.

b. Number of differential expressed genes (DEGs) in six major cell types. X-axis represents DEGs in each cell type; Y-axis represents number of DEG. A total of 69 DEGs are shared in at least two cell types, while 225 DEGs are unique for individual cell type (FDR < 0.05). Among shared DEGs in multiple cell types, up(red)- or down(blue) -regulated genes by THC are in the same direction across cell types except three DEGs (purple).

c. Violin plots showing common differentially expressed genes between pre-THC and post-THC in at least three cell types. X-axis represents cell type; Y-axis represents expression level for each gene. Blue: pre-THC samples; pink: post-THC samples.

**Figure 3 Cell-type based differential gene expression, gene-gene correlation, and biological pathways influenced delta-9-tetrahydrocannabinol**

a. Heat map showing three subtypes of CD4+ T-cells affected by THC. Color bar represents log2 fold change between post-THC and pre-THC samples. Each row represents significant genes for top 20 genes in each cell cluster. Cluster 8 shows a distinct pattern of differential gene expression from those observed in clusters 3 and 6. In cluster 8, nine genes encoding ribosomal protein are decreased in expression by THC.

b. Co-expression network in CD4+ T-cells. Genes with nominal $p<0.001$ from linear mixed regression model are selected to construct a co-expression network. Gene-gene links were derived from KEGG: Kyoto Encyclopedia of Genes and Genomes – GenomeNet. Significance is set at false discovery rate (FDR)<0.05. A total of 40 nodes and 33 edges were observed. Two hub genes, *CCR7* and *HLA-A*, are differentially expressed genes influenced by THC.

c. Heat map showing three subgroups of CD8+ T-cells affected by THC. Cluster 20 shows distinct differential gene patterns from clusters 7 and 18.

d. Co-expression network in CD8+ T-cells. Genes with nominal $p<0.001$ in CD8+ T-cells are selected to construct a co-expression network. In CD8+ T-cells, we observed 35 nodes and 31 edges. One hub gene, *HLA-A*, is differentially expressed by THC.

e. Heat map showing two subtypes of B cells affected by THC. Each row represents significant differentially expressed genes in B cells. Cluster 12 shows a distinct differential gene expression pattern from that of cluster 14.

f. Co-expression network in B cells. Genes with nominal $p<0.001$ in B cells are selected to construct a co-expression network. A total of 34 nodes and 28 edges are observed. Three hub genes, *HLA-A, HLA-DQA1*, and *HLA-DPA1* are identified.

g. Co-expression network in natural killer (NK) cells. We observe 17 nodes and 12 edges. One hub gene, *CCL4*, is significantly differentially expressed following THC infusion.

h. Heat map showing two distinct subtypes of CD14+ monocytes (cluster 10 and cluster 17) affected by THC. Color bar represents log2 fold change between pre-THC and post-THC samples. Each row represents significant genes in CD14+ monocytes.

i. Co-expression network in CD14+ monocytes. Genes with nominal $p < 0.001$ in CD4+ T-cells are selected to construct a co-expression network. We observed 18 nodes and 13 edges. One hub gene, *HLA-DQB1*, was identified in both pre-THC and post-THC samples.

j. Circus plot showing gene set enrichment analysis using KEGG annotations reveal 39 biological pathways shared in at least 2 cell types. KEGG: Kyoto Encyclopedia of Genes and Genomes – GenomeNet. Significant pathway is declared at false discovery rate (FDR)< 0.05. The legend is the name of each pathway corresponding to each spoke of the circular plot.

**Figure 4. THC receptor gene expression and co-expression network in B cells**

a. tSNE plot showing THC receptor gene expression in distinct cell types of peripheral blood mononuclear cells. *CNR1* is observed little expression in any cell types. *CNR2* is highly expressed in B cells, followed by nature killer cells, CD8+ T-cells, and minimally expressed in CD4+ T-cells. *GPR55* is highly expressed in CD4+ T-cells more than other cell types. *GPR18* is widely expressed in peripheral blood mononuclear cells.

b. *CNR2* expression is significantly correlated with 74 genes in B cells. The genes co-expressed with *CNR2* are involved in functions of biological regulation, cellular process, immune system process, metabolic process, and signal functions.

**Supplementary Figures**

**Figure S1. tSNE plot showing cell clusters after removed batch effects**

a. tSNE plot for four samples of pre- and post-THC infusion.

b. tSNE plot for pre-THC infusion of subject 1

c. tSNE plot for post-THC infusion of subject 1

d. tSNE plot for pre-THC infusion of subject 2

e. tSNE for post-THC infusion of subject 2.

**Figure S2. Sample marker gene expression in each cell type of 15,973 peripheral blood mononuclear cells**

**Figure S3. Study design and procedure of THC infusion in human subjects.**

SA: Substance Abuse; PANSS: Positive and Negative Syndrome Scale; CADSS: Clinician Administered Dissociative States Scale; VAS: Visual Analog Scale; IV: Intravenous Injection; EEG: electroencephalogram.

**Supplementary Tables**

**Table S1.** Cell markers for cell type identification

**Table S2.** Mapping cell types using generalized linear modelling

**Table S3.** Proportion of cell numbers for each sample in a given cell type

**Table S4.** A summary of the number of differentially expressed genes between post- and pre-THC samples in each cell type

**Table S5.** Differentially expressed genes affected by THC in CD4+ T-cells

**Table S6.** Differentially expressed genes affected by THC in IL7RCD4+ T-cells

**Table S7.** Differentially expressed genes affected by THC in CD8+ T-cells

**Table S8.** Differentially expressed genes affected by THC in B cells

**Table S9.** Differentially expressed genes affected by THC in natural killer cells

**Table S10.** Differentially expressed genes affected by THC in CD14+ monocytes

**Table S11.** Differentially expressed genes affected by THC in FCGR3A monocytes

**Table S12.** log2 fold change of top 20 genes between post- and pre-THC infusion in each CD4+ T-cell clusters

**Table S13**. log2 fold change of top 20 genes between post- and pre-THC infusion in each CD8+ T-cell clusters

**Table S14.** log2 fold change of top 20 genes between post- and pre-THC infusion in each B cell clusters

**Table S15.** log2 fold change of top 20 genes between post- and pre-THC infusion in each CD14+ monocytes clusters

**Table S16.** Gene Ontology (GO) term enrichment for the co-expression network in CD4+ T-cells

**Table S17.** Gene Ontology (GO) term enrichment for the co-expression network in CD8+ T-cells

**Table S18.** Gene Ontology (GO) term enrichment for the co-expression network in B cells

**Table S19.** Gene Ontology (GO) term enrichment for the co-expression network in natural killer cells

**Table S20.** Gene Ontology (GO) term enrichment for the co-expression network in CD14+ monocytes

**Table S21.** Gene Ontology (GO) term enrichment for the co-expression network in FCGR3A monocytes

**Table S22.** A summary of the number of significant pathway in each cell type

**Table S23.** Significant pathways from KEGG in CD4+ T-cells

**Table S24.** Significant pathways from KEGG in IL7RCD4+ T-cells

**Table S25.** Significant pathways from KEGG in CD8+ T-cells

**Table S26.** Significant pathways from KEGG in B cells

**Table S27.** Significant pathways from KEGG in natural killer cells

**Table S28.** Significant pathways from KEGG in CD14+ monocytes

**Table S29.** Significant pathways from KEGG in FCGR3A monocytes

**Table S30.** Pre-THC gene co-expression between *CNR2* and other genes

**Table S31.** Post-THC gene co-expression between *CNR2* and other genes

641
642 **References**
643

644 1. Katz-Talmor, D., Katz, I., Porat-Katz, B.S. & Shoenfeld, Y. Cannabinoids for the
645 treatment of rheumatic diseases - where do we stand? *Nat Rev Rheumatol* **14**, 488-498
646 (2018).
647 2. Maccarrone, M. *et al.* Endocannabinoid signaling at the periphery: 50 years after THC.
648 *Trends Pharmacol Sci* **36**, 277-96 (2015).
649 3. Tanasescu, R. & Constantinescu, C.S. Cannabinoids and the immune system: an
650 overview. *Immunobiology* **215**, 588-97 (2010).
651 4. Mackie, K. Cannabinoid receptors as therapeutic targets. *Annu Rev Pharmacol Toxicol*
652 **46**, 101-22 (2006).
653 5. Condie, R., Herring, A., Koh, W.S., Lee, M. & Kaminski, N.E. Cannabinoid inhibition of
654 adenylate cyclase-mediated signal transduction and interleukin 2 (IL-2) expression in the
655 murine T-cell line, EL4.IL-2. *J Biol Chem* **271**, 13175-83 (1996).
656 6. Turcotte, C., Blanchet, M.R., Laviolette, M. & Flamand, N. The CB2 receptor and its role
657 as a regulator of inflammation. *Cell Mol Life Sci* **73**, 4449-4470 (2016).
658 7. Nahas, G.G., Zagury, D., Schwartz, I.W. & Nagel, M.D. Evidence for the possible
659 immunogenicity of delta 9-tetrahydrocannabinol (THC) in rodents. *Nature* **243**, 407-8
660 (1973).
661 8. Croxford, J.L. & Yamamura, T. Cannabinoids and the immune system: potential for the
662 treatment of inflammatory diseases? *J Neuroimmunol* **166**, 3-18 (2005).
663 9. Nahas, G.G., Morishima, A. & Desoize, B. Effects of cannabinoids on macromolecular
664 synthesis and replication of cultured lymphocytes. *Fed Proc* **36**, 1748-52 (1977).

10. McKallip, R.J., Nagarkatti, M. & Nagarkatti, P.S. Delta-9-tetrahydrocannabinol enhances breast cancer growth and metastasis by suppression of the antitumor immune response. *J Immunol* **174**, 3281-9 (2005).

11. Yuan, M. *et al.* Delta 9-Tetrahydrocannabinol regulates Th1/Th2 cytokine balance in activated human T cells. *J Neuroimmunol* **133**, 124-31 (2002).

12. Herrera, B. *et al.* The CB2 cannabinoid receptor signals apoptosis via ceramide-dependent activation of the mitochondrial intrinsic pathway. *Exp Cell Res* **312**, 2121-31 (2006).

13. Jia, W. *et al.* Delta9-tetrahydrocannabinol-induced apoptosis in Jurkat leukemia T cells is regulated by translocation of Bad to mitochondria. *Mol Cancer Res* **4**, 549-62 (2006).

14. Shalek, A.K. *et al.* Single-cell transcriptomics reveals bimodality in expression and splicing in immune cells. *Nature* **498**, 236-40 (2013).

15. Wills, Q.F. *et al.* Single-cell gene expression analysis reveals genetic associations masked in whole-tissue experiments. *Nat Biotechnol* **31**, 748-52 (2013).

16. Stubbington, M.J.T., Rozenblatt-Rosen, O., Regev, A. & Teichmann, S.A. Single-cell transcriptomics to explore the immune system in health and disease. *Science* **358**, 58-63 (2017).

17. Mathys, H. *et al.* Single-cell transcriptomic analysis of Alzheimer's disease. *Nature* (2019).

18. D'Souza, D.C. *et al.* The Psychotomimetic Effects of Intravenous Delta-9-Tetrahydrocannabinol in Healthy Individuals: Implications for Psychosis. *Neuropsychopharmacology* **29**, 1558 (2004).

19. Carbuto, M. *et al.* The safety of studies with intravenous Delta(9)-tetrahydrocannabinol in humans, with case histories. *Psychopharmacology (Berl)* **219**, 885-96 (2012).

20. Boggs, D.L. *et al.* The dose-dependent psychomotor effects of intravenous delta-9-tetrahydrocannabinol (Delta(9)-THC) in humans. *J Psychopharmacol* **32**, 1308-1318 (2018).

21. Sherif, M., Radhakrishnan, R., D'Souza, D.C. & Ranganathan, M. Human Laboratory Studies on Cannabinoids and Psychosis. *Biol Psychiatry* **79**, 526-38 (2016).

22. Zheng, G.X. *et al.* Massively parallel digital transcriptional profiling of single cells. *Nat Commun* **8**, 14049 (2017).

23. Butler, A., Hoffman, P., Smibert, P., Papalexi, E. & Satija, R. Integrating single-cell transcriptomic data across different conditions, technologies, and species. *Nature Biotechnology* **36**, 411 (2018).

24. Leek, J.T. & Storey, J.D. Capturing heterogeneity in gene expression studies by surrogate variable analysis. *PLoS Genet* **3**, 1724-35 (2007).

25. Schelker, M. *et al.* Estimation of immune cell content in tumour tissue using single-cell RNA-seq data. *Nat Commun* **8**, 2032 (2017).

26. Gebhardt, C., Nemeth, J., Angel, P. & Hess, J. S100A8 and S100A9 in inflammation and cancer. *Biochem Pharmacol* **72**, 1622-31 (2006).

27. Riva, M. *et al.* Induction of nuclear factor-kappaB responses by the S100A9 protein is Toll-like receptor-4-dependent. *Immunology* **137**, 172-82 (2012).

28. Champaiboon, C., Sappington, K.J., Guenther, B.D., Ross, K.F. & Herzberg, M.C. Calprotectin S100A9 calcium-binding loops I and II are essential for keratinocyte resistance to bacterial invasion. *J Biol Chem* **284**, 7078-90 (2009).

29. Tewary, P. *et al.* Granulysin activates antigen-presenting cells through TLR4 and acts as an immune alarmin. *Blood* **116**, 3465-74 (2010).

30. El-Gohary, M. & Eid, M.A. Effect of cannabinoid ingestion (in the form of bhang) on the immune system of high school and university students. *Hum Exp Toxicol* **23**, 149-56 (2004).

31. Eisenstein, T.K., Meissler, J.J., Wilson, Q., Gaughan, J.P. & Adler, M.W. Anandamide and Delta9-tetrahydrocannabinol directly inhibit cells of the immune system via CB2 receptors. *J Neuroimmunol* **189**, 17-22 (2007).

32. Lu, T., Newton, C., Perkins, I., Friedman, H. & Klein, T.W. Cannabinoid treatment suppresses the T-helper cell-polarizing function of mouse dendritic cells stimulated with Legionella pneumophila infection. *J Pharmacol Exp Ther* **319**, 269-76 (2006).

33. Massi, P., Vaccani, A. & Parolaro, D. Cannabinoids, immune system and cytokine network. *Curr Pharm Des* **12**, 3135-46 (2006).

34. Winkler, G.S. The mammalian anti-proliferative BTG/Tob protein family. *J Cell Physiol* **222**, 66-72 (2010).

35. Sofer, A., Lei, K., Johannessen, C.M. & Ellisen, L.W. Regulation of mTOR and cell growth in response to energy stress by REDD1. *Mol Cell Biol* **25**, 5834-45 (2005).

36. Zhang, X. *et al.* Thymosin beta 10 is a key regulator of tumorigenesis and metastasis and a novel serum marker in breast cancer. *Breast Cancer Res* **19**, 15 (2017).

37. Tabb-Massey, A. *et al.* Ribosomal proteins Rps0 and Rps21 of Saccharomyces cerevisiae have overlapping functions in the maturation of the 3' end of 18S rRNA. *Nucleic Acids Res* **31**, 6798-805 (2003).

38. Wang, A. *et al.* Ribosomal protein RPL41 induces rapid degradation of ATF4, a transcription factor critical for tumour cell survival in stress. *J Pathol* **225**, 285-92 (2011).

39. Kanehisa, M. & Goto, S. KEGG: kyoto encyclopedia of genes and genomes. *Nucleic Acids Res* **28**, 27-30 (2000).

40. Zhu, W., Newton, C., Daaka, Y., Friedman, H. & Klein, T.W. delta 9-Tetrahydrocannabinol enhances the secretion of interleukin 1 from endotoxin-stimulated macrophages. *J Pharmacol Exp Ther* **270**, 1334-9 (1994).

41. Albig, W. *et al.* The human replacement histone H3.3B gene (H3F3B). *Genomics* **30**, 264-72 (1995).

42. Li, C. *et al.* Mutational landscape of primary, metastatic, and recurrent ovarian cancer reveals c-MYC gains as potential target for BET inhibitors. *Proc Natl Acad Sci U S A* **116**, 619-624 (2019).

43. Kim, D.H. *et al.* Intracellular interleukin-32gamma mediates antiviral activity of cytokines against hepatitis B virus. *Nat Commun* **9**, 3284 (2018).

44. Yoshimura, A., Suzuki, M., Sakaguchi, R., Hanada, T. & Yasukawa, H. SOCS, Inflammation, and Autoimmunity. *Front Immunol* **3**, 20 (2012).

45. Mamane, Y. *et al.* Interferon regulatory factors: the next generation. *Gene* **237**, 1-14 (1999).

46. Shirasawa, T. *et al.* A novel gene product associated with mu chains in immature B cells. *EMBO J* **12**, 1827-34 (1993).

47. Toutenhoofd, S.L. *et al.* Characterization of the human CALM2 calmodulin gene and comparison of the transcriptional activity of CALM1, CALM2 and CALM3. *Cell Calcium* **23**, 323-38 (1998).

48. Divanovic, S. *et al.* Negative regulation of Toll-like receptor 4 signaling by the Toll-like receptor homolog RP105. *Nat Immunol* **6**, 571-8 (2005).

49. Shah, S., King, E.M., Chandrasekhar, A. & Newton, R. Roles for the mitogen-activated protein kinase (MAPK) phosphatase, DUSP1, in feedback control of inflammatory gene expression and repression by dexamethasone. *J Biol Chem* **289**, 13667-79 (2014).

50. Lee, S.F., Newton, C., Widen, R., Friedman, H. & Klein, T.W. Differential expression of cannabinoid CB(2) receptor mRNA in mouse immune cell subpopulations and following B cell stimulation. *Eur J Pharmacol* **423**, 235-41 (2001).

51. Lauckner, J.E. *et al.* GPR55 is a cannabinoid receptor that increases intracellular calcium and inhibits M current. *Proc Natl Acad Sci U S A* **105**, 2699-704 (2008).

52. Spitzer, R.L., Davies, M. & Barkley, R.A. The DSM-III-R field trial of disruptive behavior disorders. *J Am Acad Child Adolesc Psychiatry* **29**, 690-7 (1990).

53. Agurell, S. *et al.* Pharmacokinetics and metabolism of delta 1-tetrahydrocannabinol and other cannabinoids with emphasis on man. *Pharmacol Rev* **38**, 21-43 (1986).

54. Volkow, N.D., Fowler, J.S., Wolf, A.P. & Gillespi, H. Metabolic studies of drugs of abuse. *NIDA Res Monogr* **105**, 47-53 (1990).

55. Volkow, N.D. *et al.* Brain glucose metabolism in chronic marijuana users at baseline and during marijuana intoxication. *Psychiatry Res* **67**, 29-38 (1996).

56. Azorlosa, J.L., Heishman, S.J., Stitzer, M.L. & Mahaffey, J.M. Marijuana smoking: effect of varying delta 9-tetrahydrocannabinol content and number of puffs. *J Pharmacol Exp Ther* **261**, 114-22 (1992).

57. Huang, D.W. *et al.* The DAVID Gene Functional Classification Tool: a novel biological module-centric algorithm to functionally analyze large gene lists. *Genome Biol* **8**, R183 (2007).

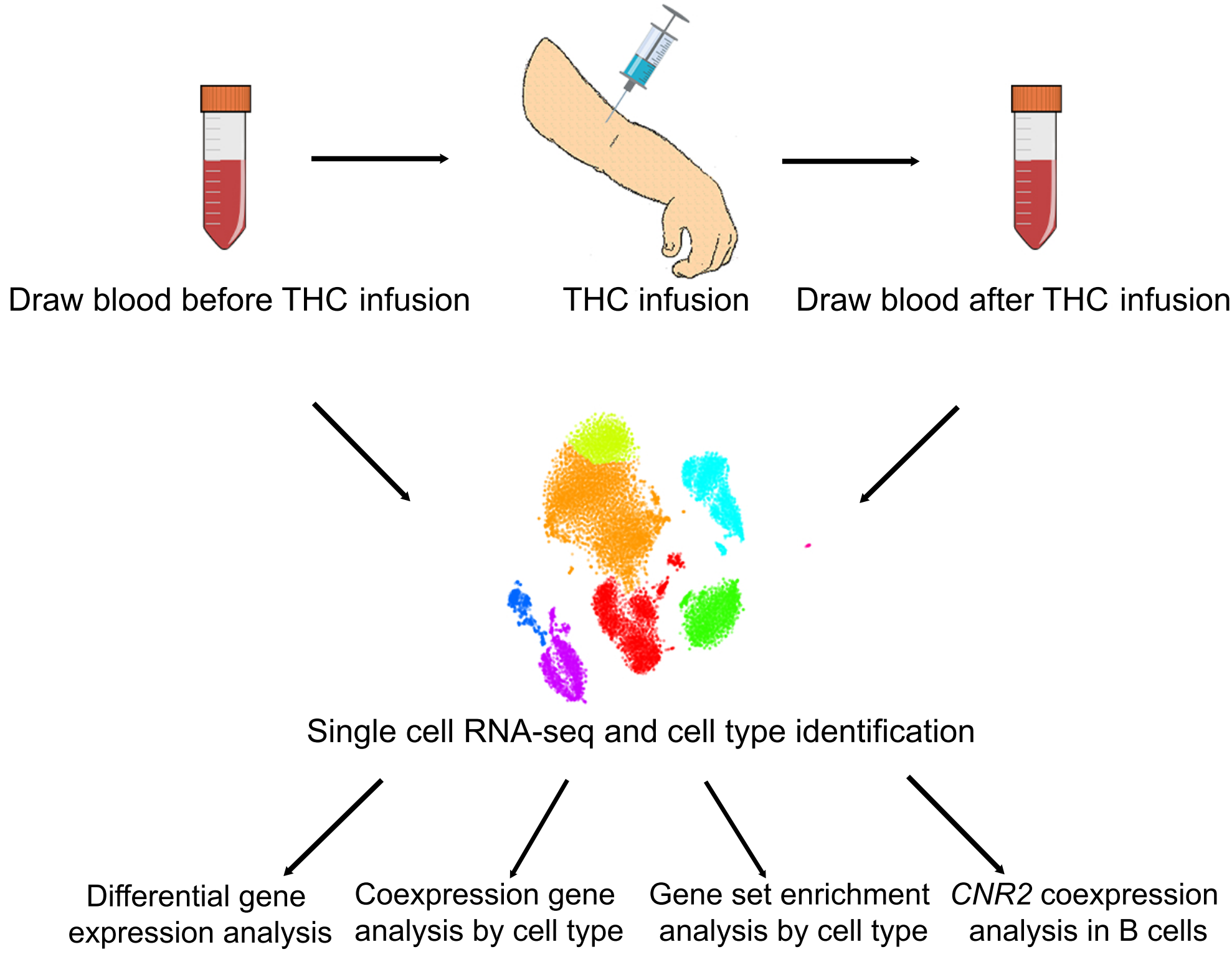
Draw blood before THC infusion
THC infusion
Draw blood after THC infusion
Single cell RNA-seq and cell type identification
Differential gene expression analysis
Coexpression gene analysis by cell type
Gene set enrichment analysis by cell type
CNR2 coexpression analysis in B cells

**Figure 1a**

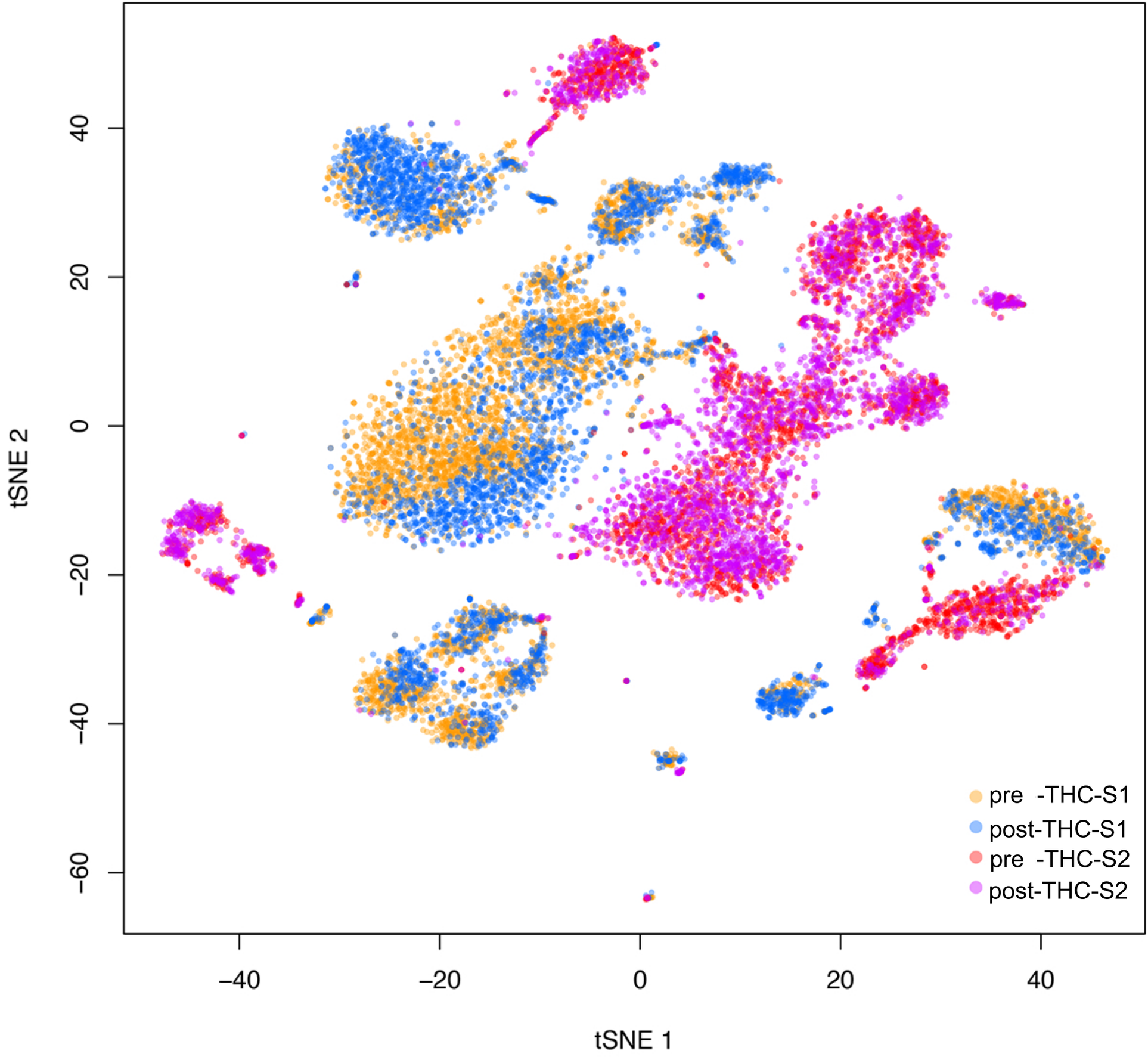
tSNE 2
40
20
0
−20
−40
−60
−40
−20
0
20
40
tSNE 1
pre -THC-S1
post-THC-S1
pre -THC-S2
post-THC-S2

**Figure 1b**

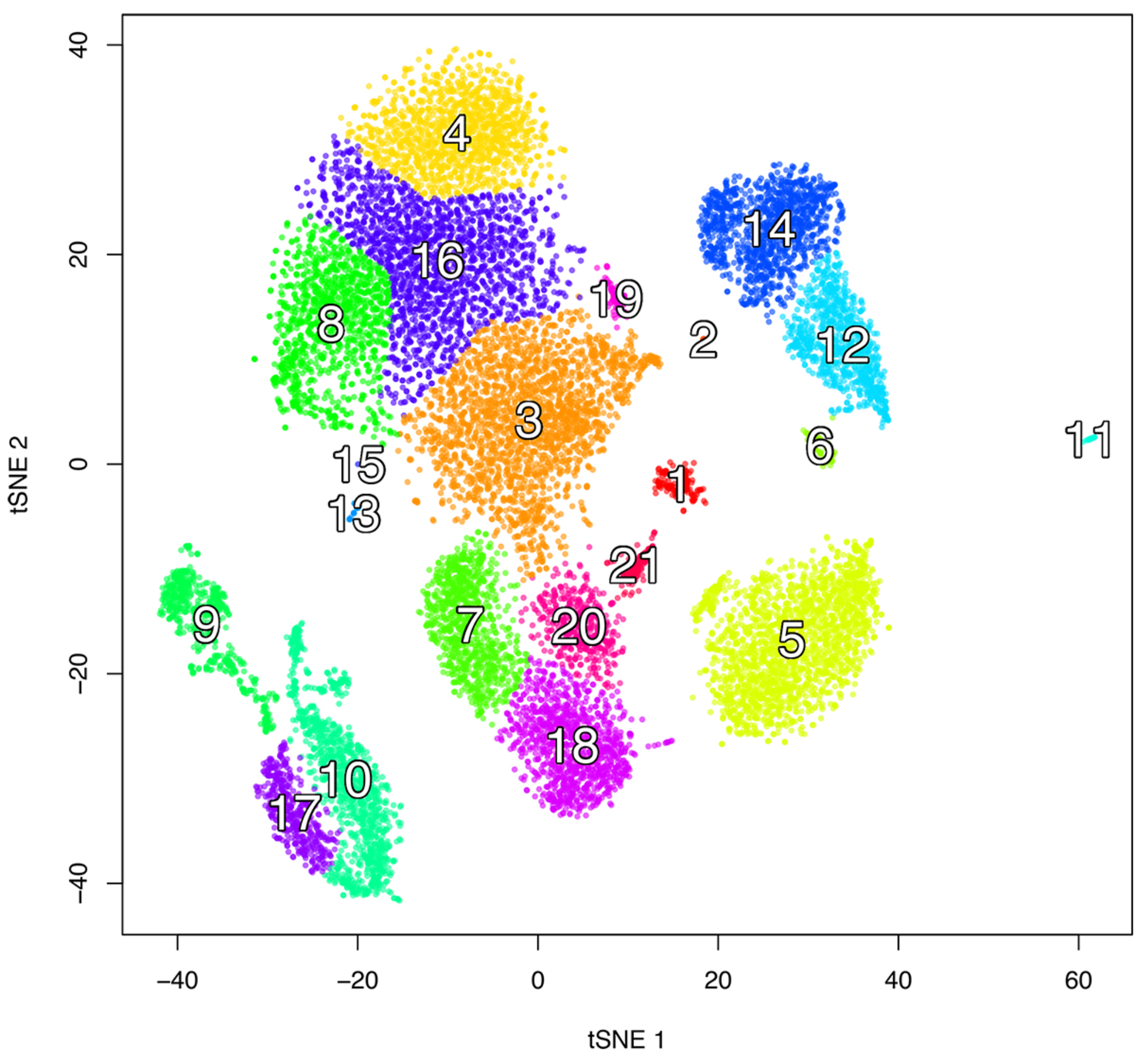
4
16
14
19
8
2
12
3
6
11
15
1
13
21
9
7
20
5
18
10
17
tSNE 2
tSNE 1
40
20
0
−20
−40
−40
−20
0
20
40
60

**Figure 1c**

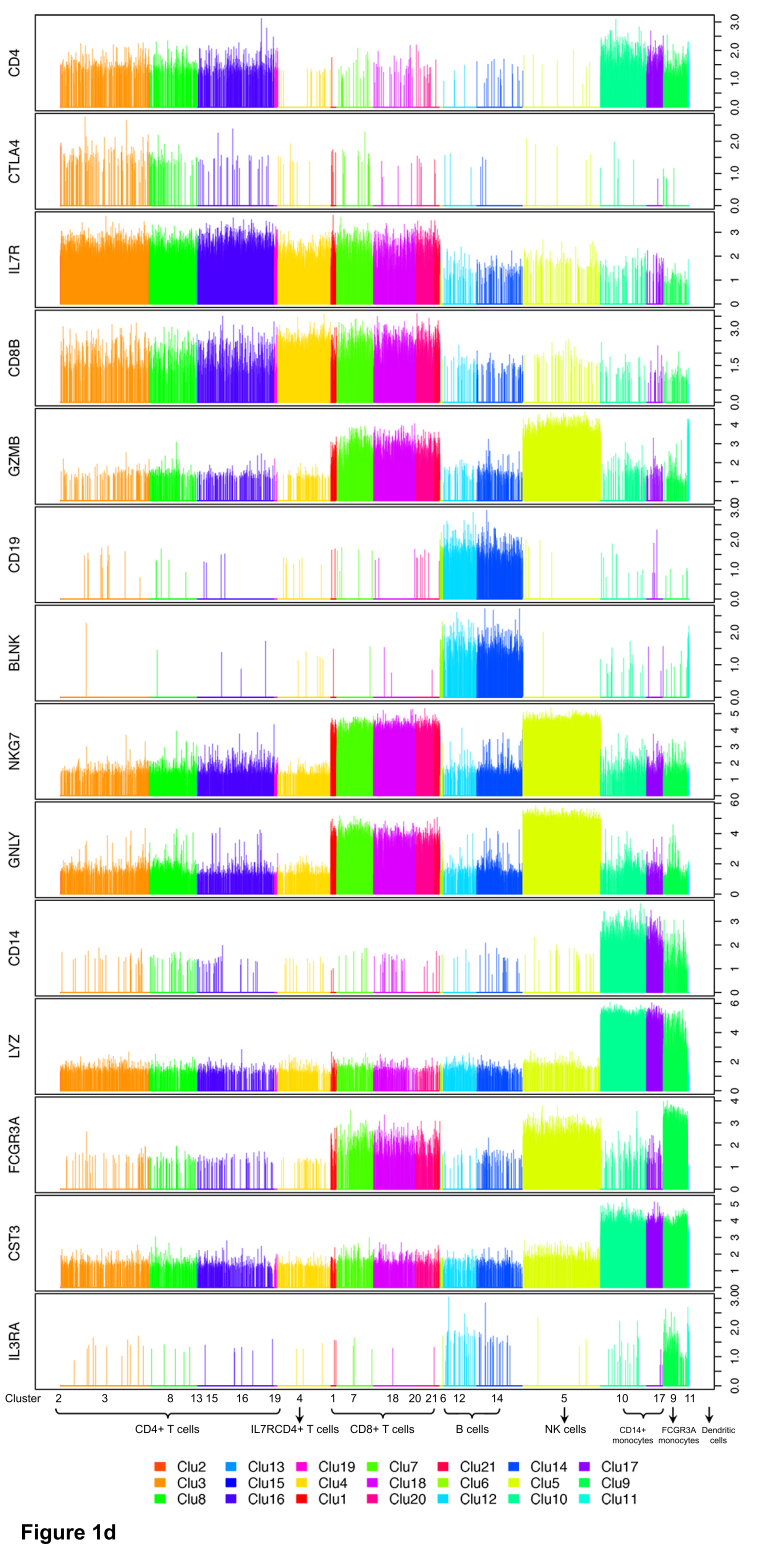
CD4
CTLA4
IL7R
CD8B
GZMB
CD19
BLNK
NKG7
GNLY
CD14
LYZ
FCGR3A
CST3
IL3RA
Cluster
2 3 8 13 15 16 19 4 1 7 18 20 21 6 12 14 5 10 17 9 11
CD4+ T cells
IL7RCD4+ T cells
CD8+ T cells
B cells
NK cells
CD14+ monocytes
FCGR3A monocytes
Dendritic cells
Clu2
Clu3
Clu8
Clu13
Clu15
Clu16
Clu19
Clu4
Clu1
Clu7
Clu18
Clu20
Clu21
Clu6
Clu12
Clu14
Clu5
Clu10
Clu17
Clu9
Clu11

**Figure 1d**

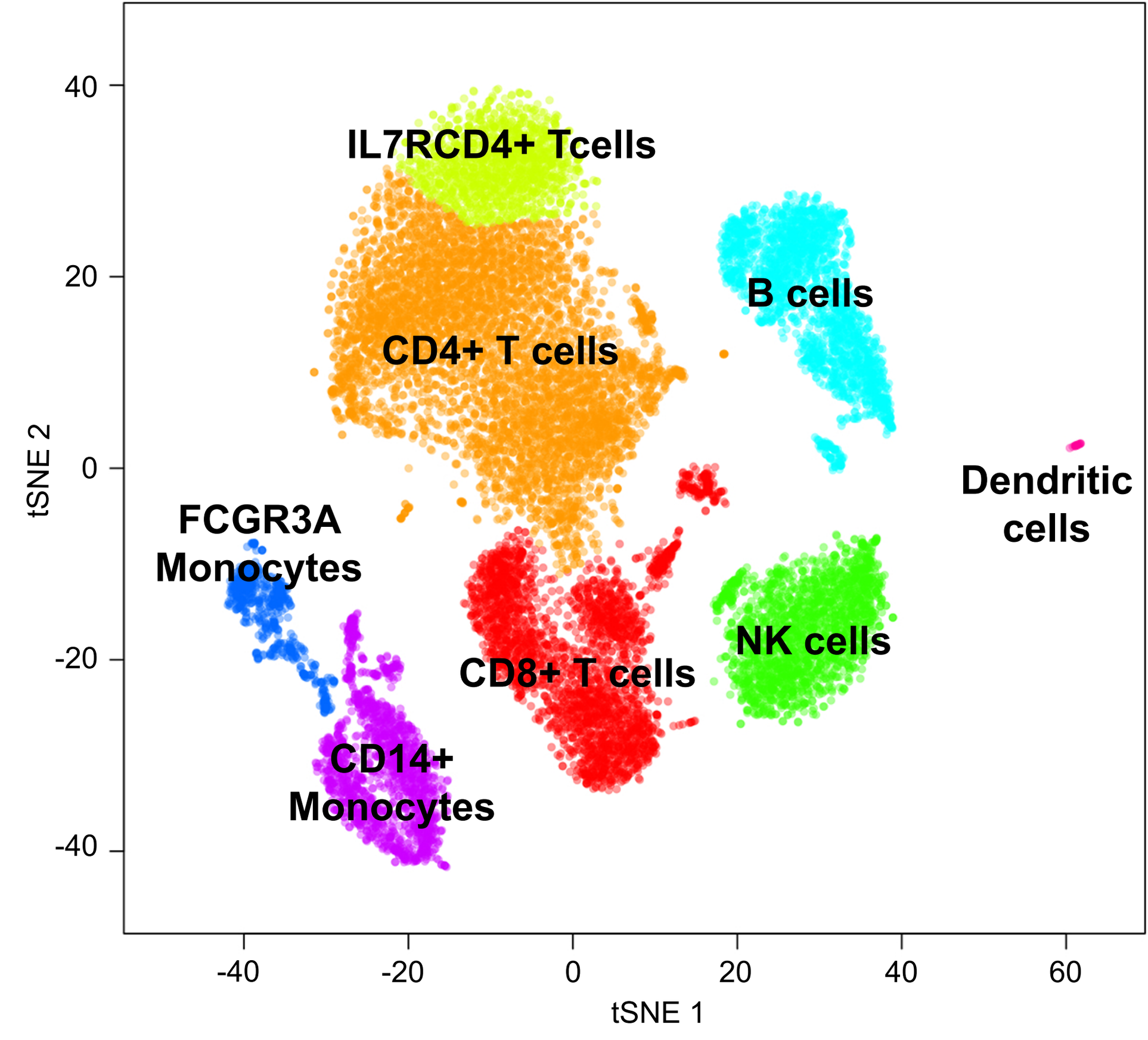
IL7RCD4+ Tcells
CD4+ T cells
B cells
Dendritic cells
FCGR3A Monocytes
NK cells
CD8+ T cells
CD14+ Monocytes
tSNE 1
tSNE 2
40
20
0
-20
-40
-40
-20
0
20
40
60

**Figure 1e**

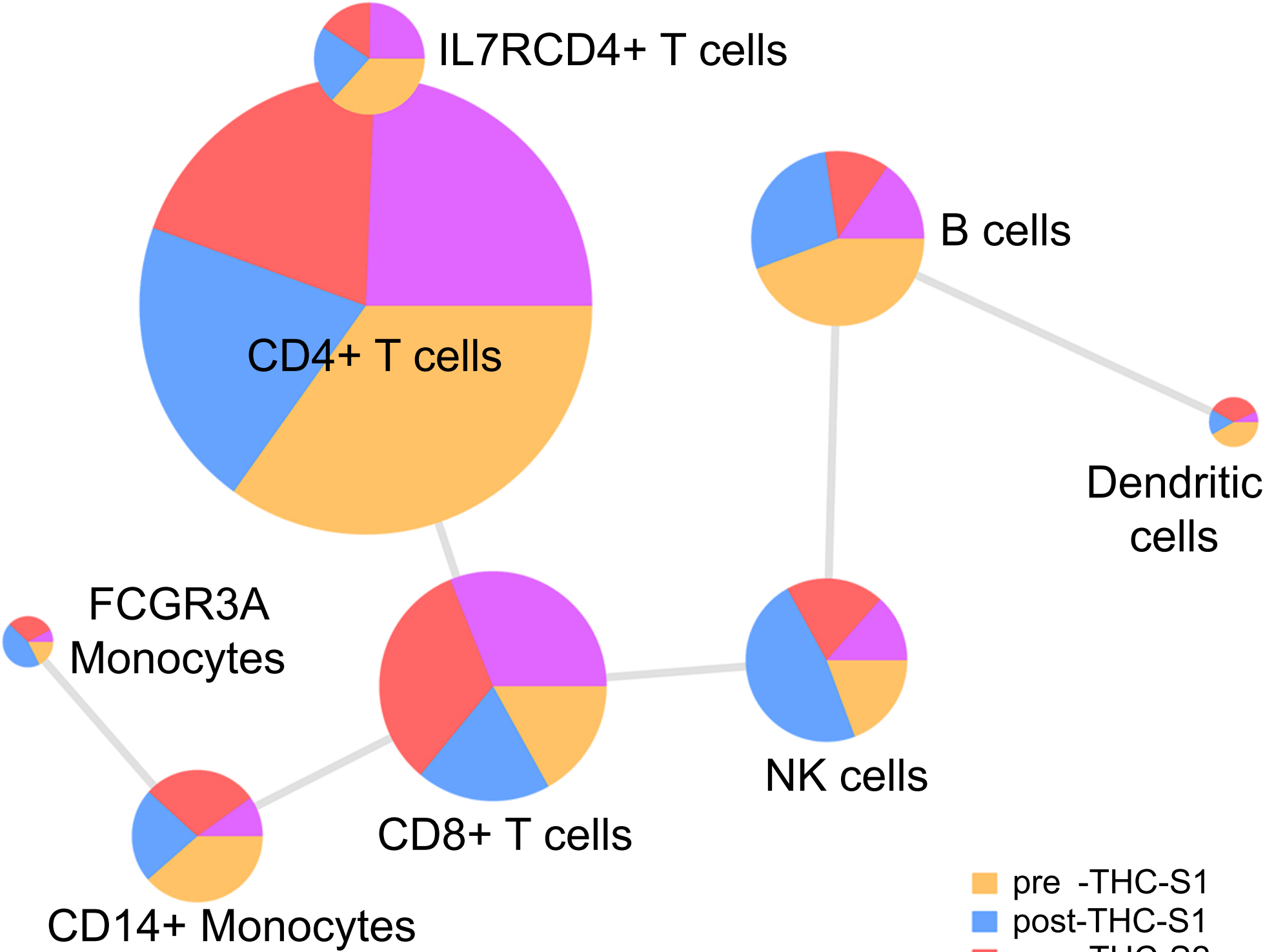
IL7RCD4+ T cells
B cells
CD4+ T cells
Dendritic cells
FCGR3A Monocytes
CD8+ T cells
NK cells
CD14+ Monocytes
pre -THC-S1
post-THC-S1
pre -THC-S2
post-THC-S2

**Figure 1f**

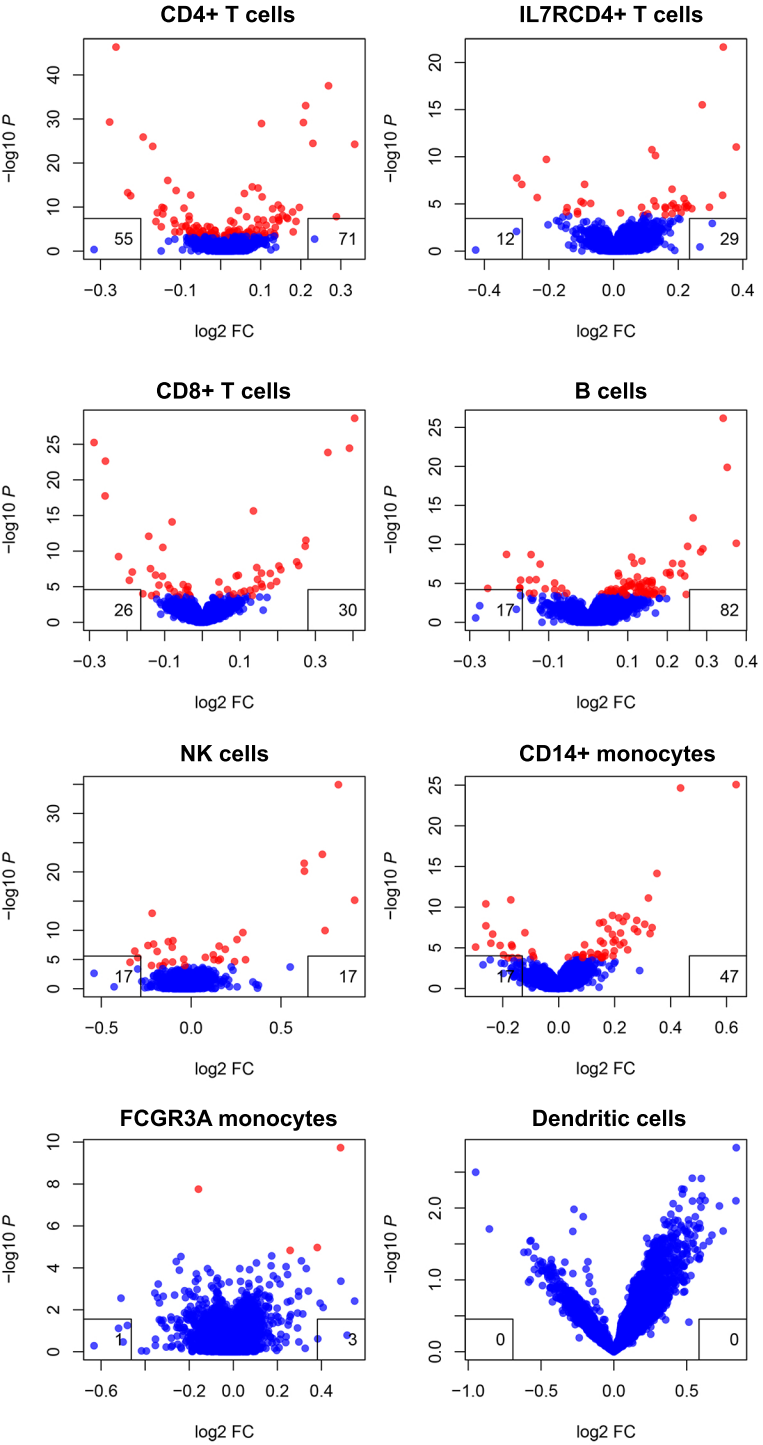
CD4+ T cells
55
71
log2 FC
−log10 P
IL7RCD4+ T cells
12
29
log2 FC
−log10 P
CD8+ T cells
26
30
log2 FC
−log10 P
B cells
17
82
log2 FC
−log10 P
NK cells
17
17
log2 FC
−log10 P
CD14+ monocytes
17
47
log2 FC
−log10 P
FCGR3A monocytes
1
3
log2 FC
−log10 P
Dendritic cells
0
0
log2 FC
−log10 P

**Figure 2a**

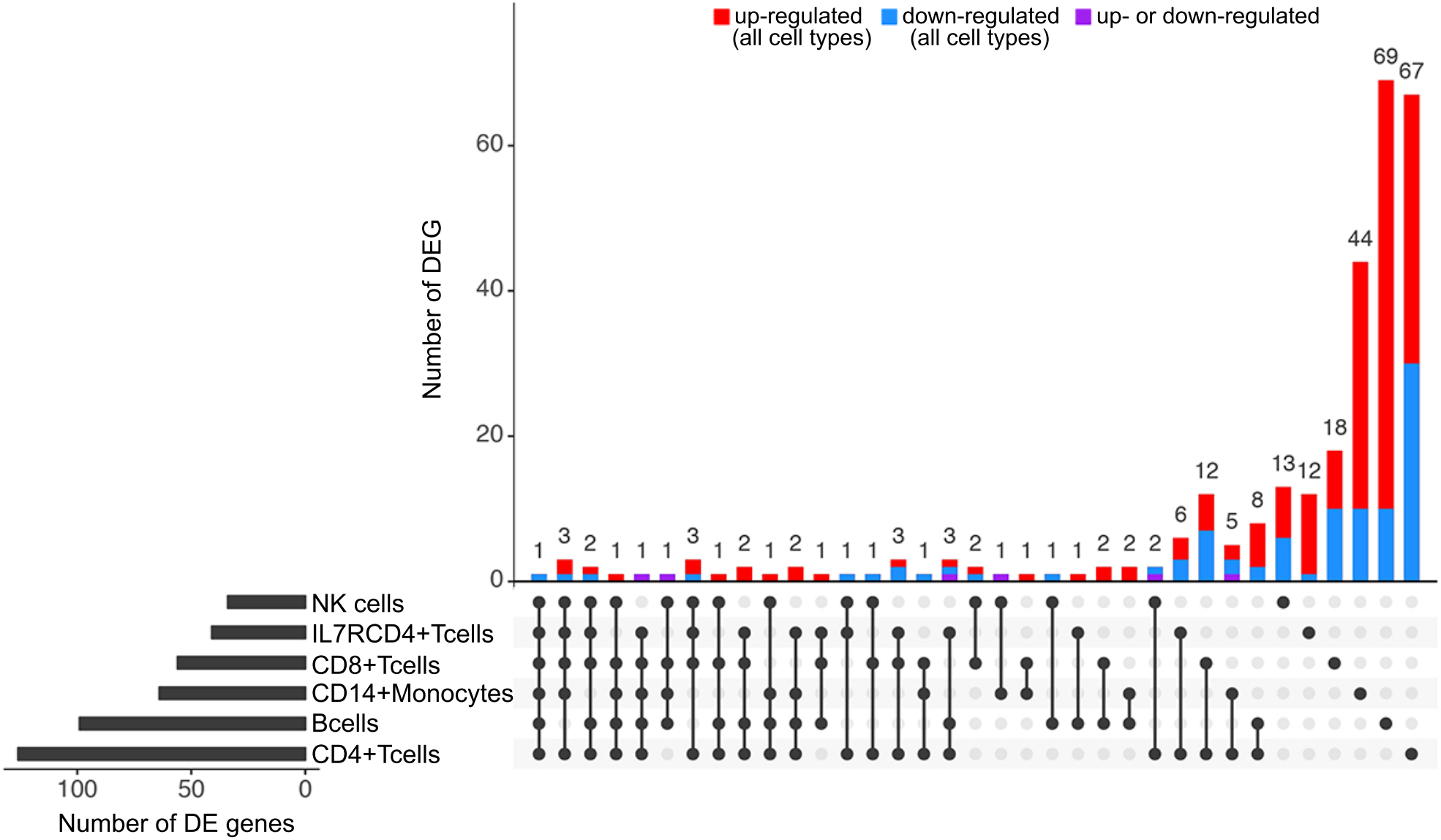
up-regulated (all cell types)
down-regulated (all cell types)
up- or down-regulated
Number of DEG
0
20
40
60
1 3 2 1 1 1 3 1 2 1 2 1 1 1 3 1 3 2 1 1 1 1 2 2 2 6 12 5 8 13 12 18 44 69 67
NK cells
IL7RCD4+Tcells
CD8+Tcells
CD14+Monocytes
Bcells
CD4+Tcells
100
50
0
Number of DE genes

**Figure 2b**

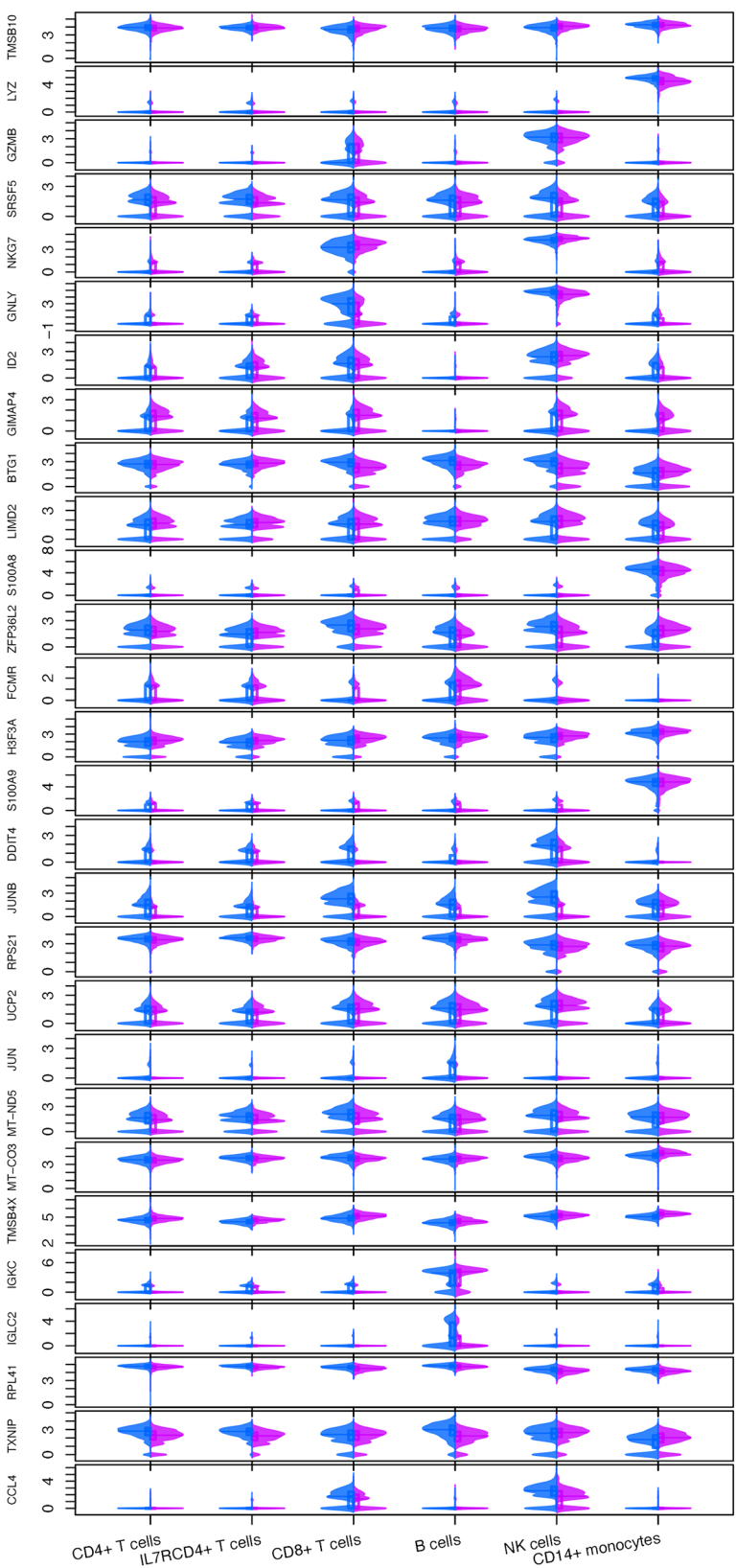
TMSB10
LYZ
GZMB
SRSF5
NKG7
GNLY
ID2
GIMAP4
BTG1
LIMD2
S100A8
ZFP36L2
FCMR
H3F3A
S100A9
DDIT4
JUNB
RPS21
UCP2
JUN
MT-ND5
MT-CO3
TMSB4X
IGKC
IGLC2
RPL41
TXNIP
CCL4
CD4+ T cells
IL7RCD4+ T cells
CD8+ T cells
B cells
NK cells
CD14+ monocytes

**Figure 2c**

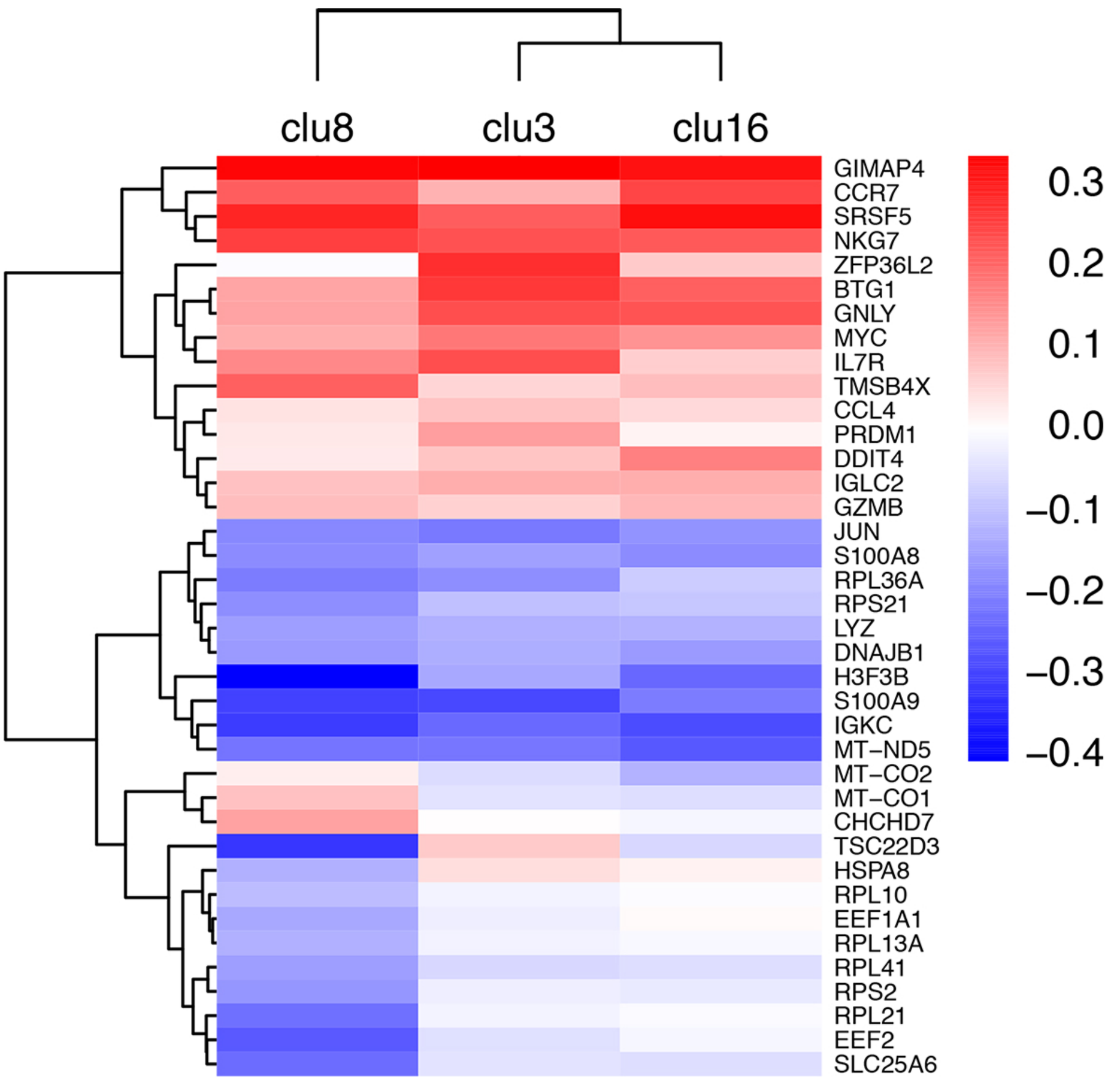
clu8
clu3
clu16
GIMAP4
CCR7
SRSF5
NKG7
ZFP36L2
BTG1
GNLY
MYC
IL7R
TMSB4X
CCL4
PRDM1
DDIT4
IGLC2
GZMB
JUN
S100A8
RPL36A
RPS21
LYZ
DNAJB1
H3F3B
S100A9
IGKC
MT−ND5
MT−CO2
MT−CO1
CHCHD7
TSC22D3
HSPA8
RPL10
EEF1A1
RPL13A
RPL41
RPS2
RPL21
EEF2
SLC25A6
0.3
0.2
0.1
0.0
−0.1
−0.2
−0.3
−0.4

**Figure 3a**

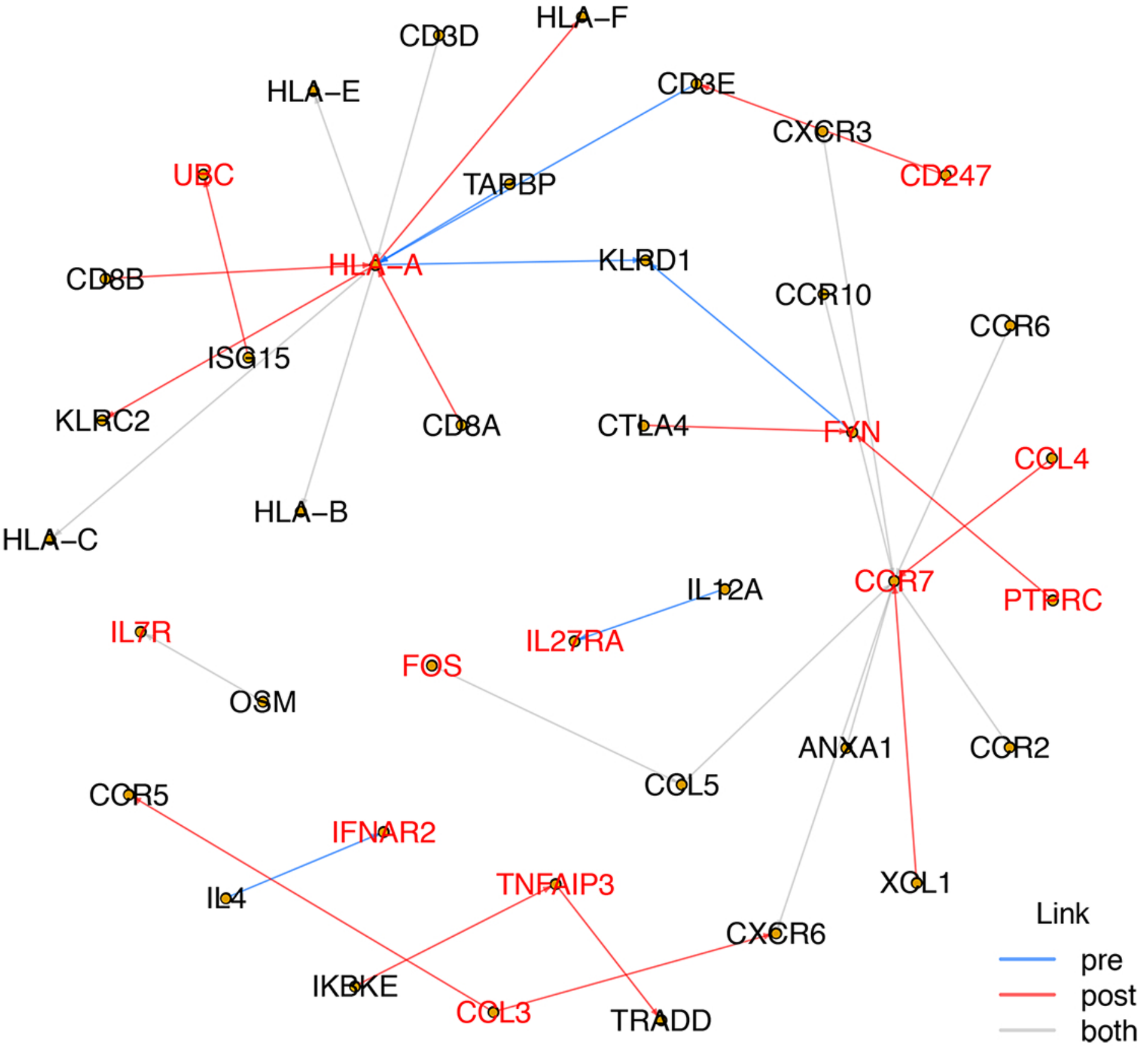
HLA−F
CD3D
HLA−E
CD3E
CXCR3
UBC
TAPBP
CD247
HLA−A
KLRD1
CD8B
CCR10
CCR6
ISG15
KLRC2
CD8A
CTLA4
FYN
CCL4
HLA−B
HLA−C
CCR7
IL12A
PTPRC
IL7R
IL27RA
FOS
OSM
ANXA1
CCR2
CCL5
CCR5
IFNAR2
XCL1
TNFAIP3
IL4
CXCR6
IKBKE
CCL3
TRADD
Link
pre
post
both

**Figure 3b**

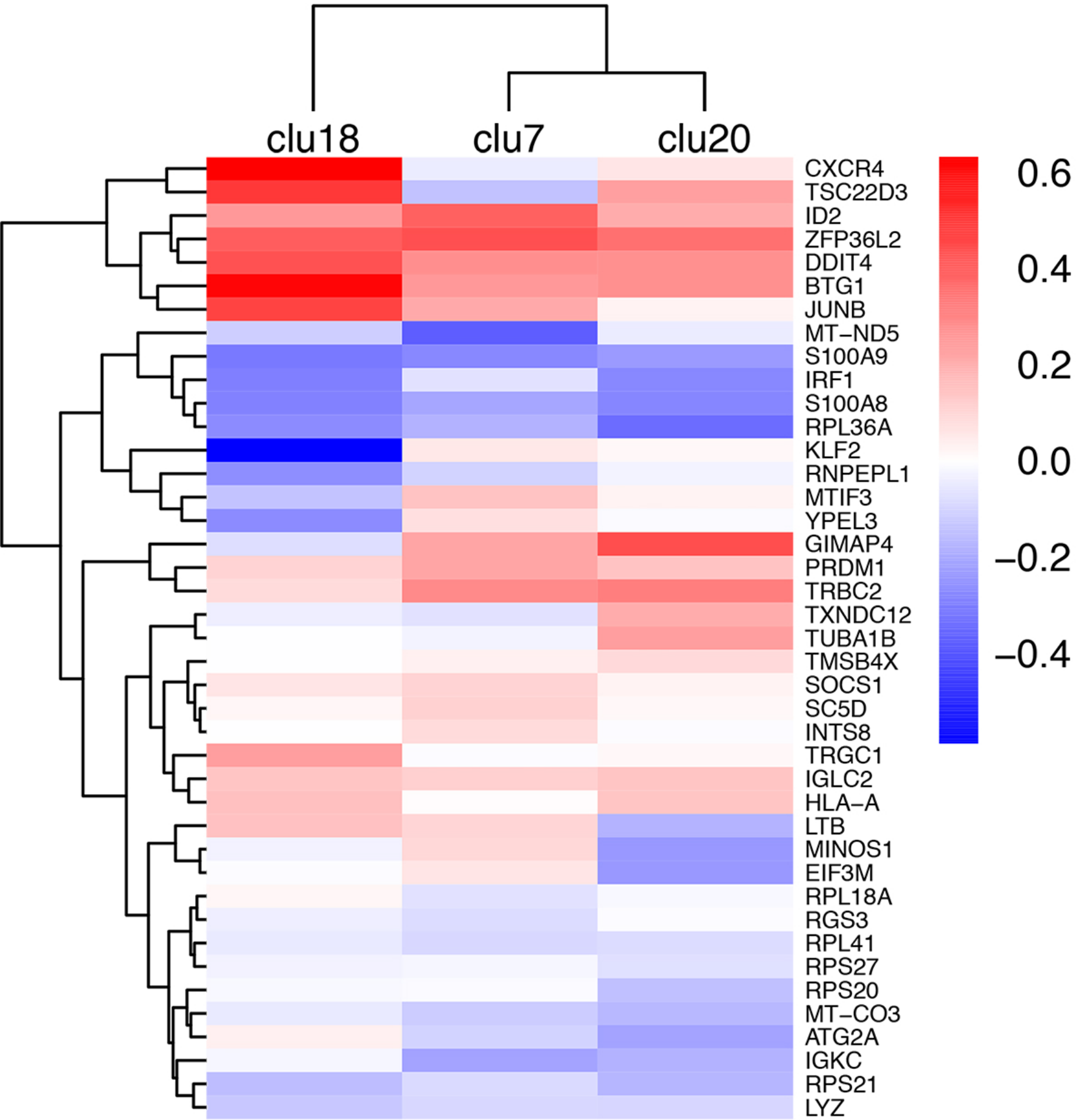
clu18
clu7
clu20
CXCR4
TSC22D3
ID2
ZFP36L2
DDIT4
BTG1
JUNB
MT−ND5
S100A9
IRF1
S100A8
RPL36A
KLF2
RNPEPL1
MTIF3
YPEL3
GIMAP4
PRDM1
TRBC2
TXNDC12
TUBA1B
TMSB4X
SOCS1
SC5D
INTS8
TRGC1
IGLC2
HLA−A
LTB
MINOS1
EIF3M
RPL18A
RGS3
RPL41
RPS27
RPS20
MT−CO3
ATG2A
IGKC
RPS21
LYZ
0.6
0.4
0.2
0.0
−0.2
−0.4

**Figure 3c**

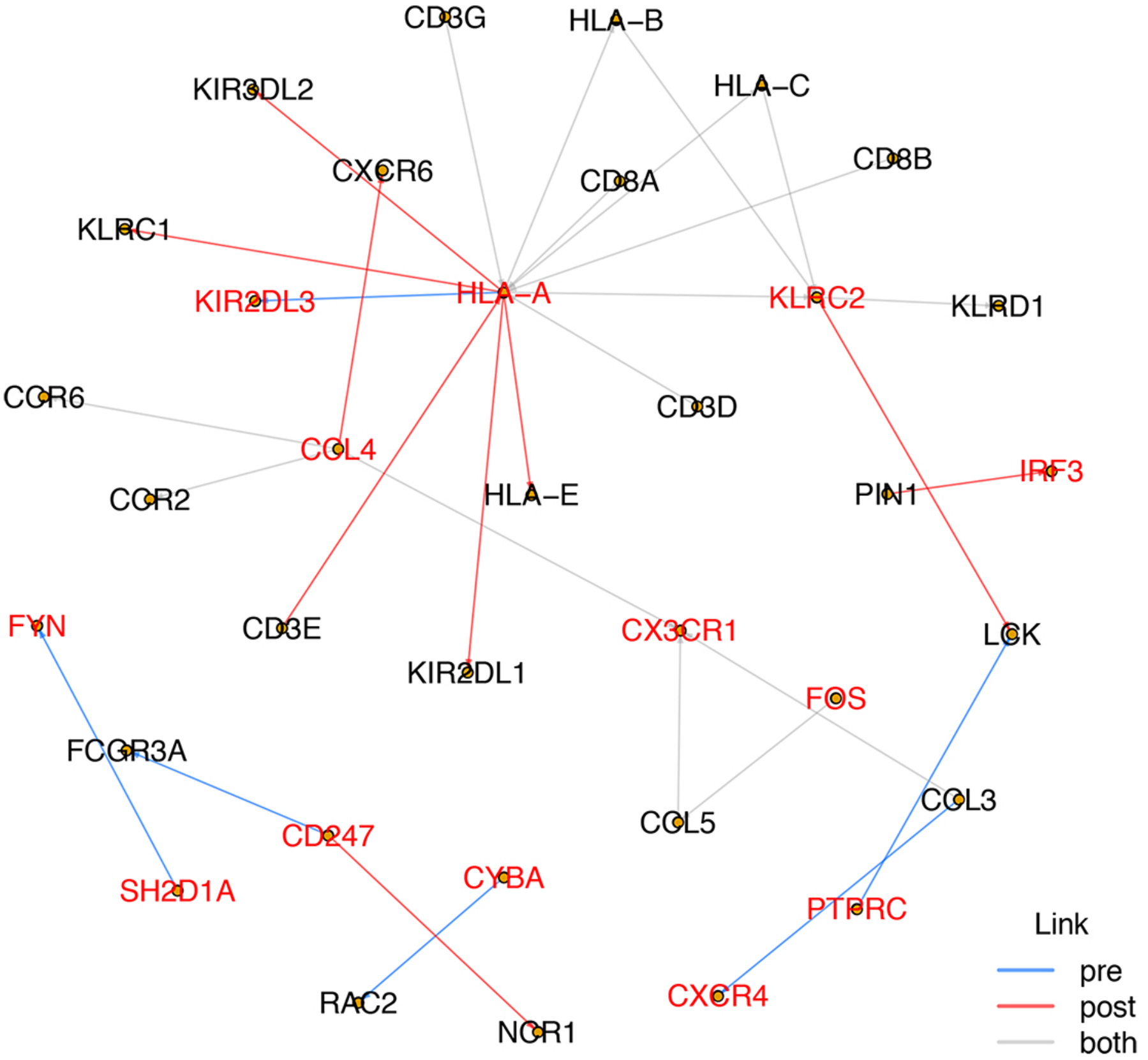
CD3G
HLA−B
KIR3DL2
HLA−C
CXCR6
CD8B
CD8A
KLRC1
KIR2DL3
HLA−A
KLRC2
KLRD1
CCR6
CD3D
CCL4
IRF3
CCR2
HLA−E
PIN1
FYN
CD3E
CX3CR1
LCK
KIR2DL1
FOS
FCGR3A
CCL3
CCL5
CD247
SH2D1A
CYBA
PTPRC
RAC2
CXCR4
NCR1
Link
pre
post
both

**Figure 3d**

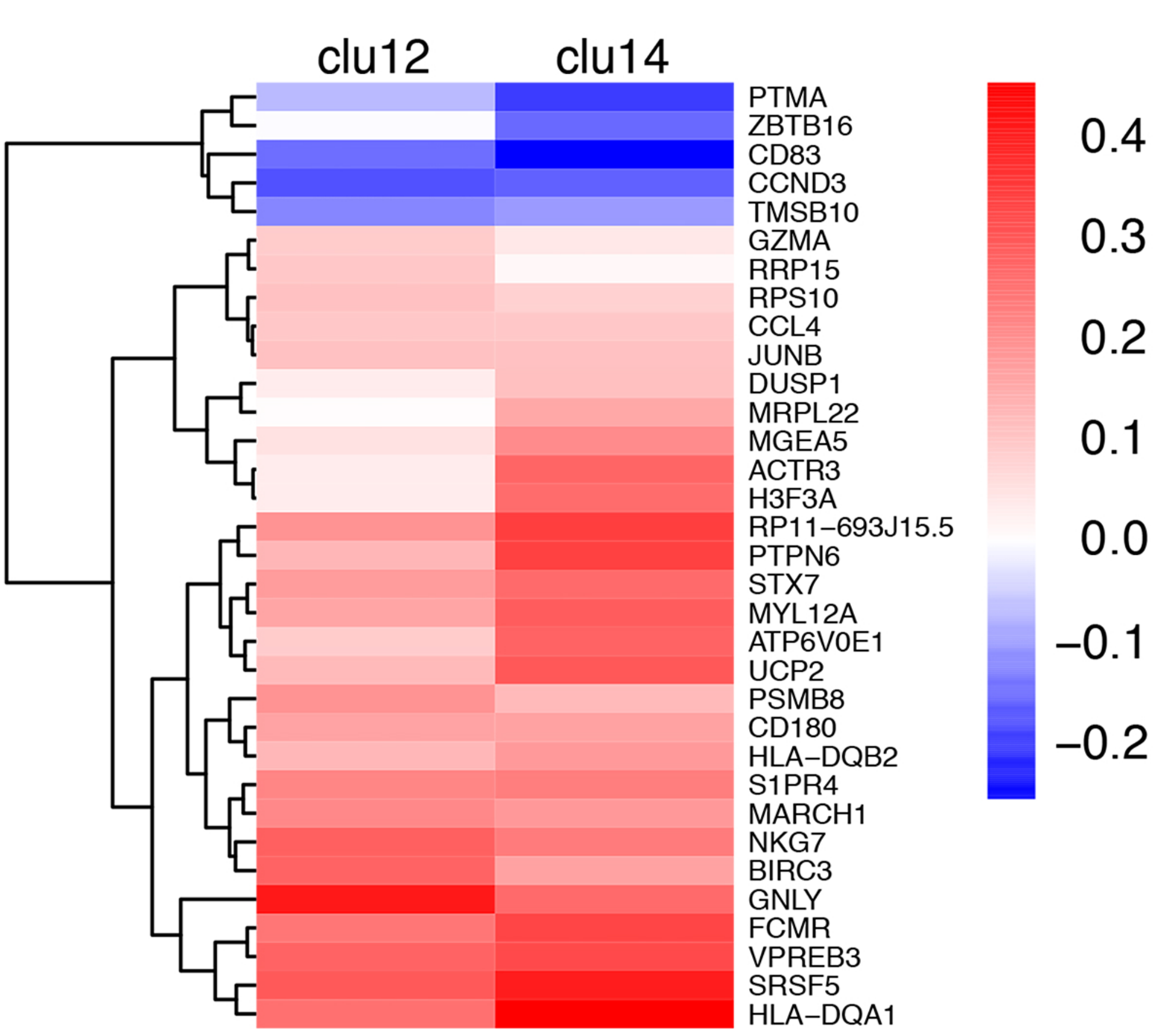
clu12
clu14
PTMA
ZBTB16
CD83
CCND3
TMSB10
GZMA
RRP15
RPS10
CCL4
JUNB
DUSP1
MRPL22
MGEA5
ACTR3
H3F3A
RP11−693J15.5
PTPN6
STX7
MYL12A
ATP6V0E1
UCP2
PSMB8
CD180
HLA−DQB2
S1PR4
MARCH1
NKG7
BIRC3
GNLY
FCMR
VPREB3
SRSF5
HLA−DQA1
0.4
0.3
0.2
0.1
0.0
−0.1
−0.2

**Figure 3e**

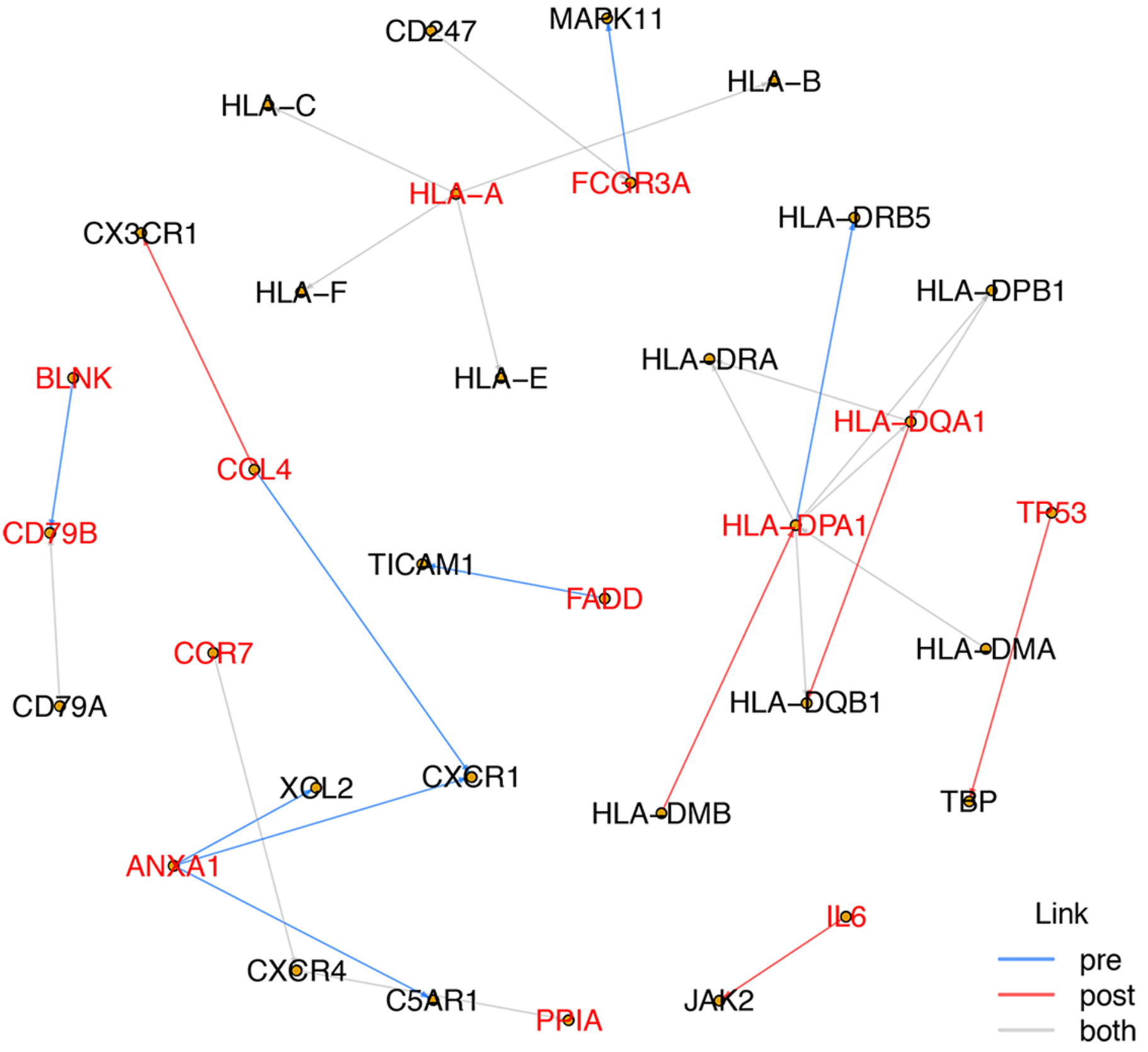
CD247
MAPK11
HLA−B
HLA−C
HLA−A
FCGR3A
HLA−DRB5
CX3CR1
HLA−F
HLA−DPB1
HLA−DRA
BLNK
HLA−E
HLA−DQA1
COL4
TP53
HLA−DPA1
CD79B
TICAM1
FADD
HLA−DMA
CCR7
CD79A
HLA−DQB1
CXCR1
XCL2
TBP
HLA−DMB
ANXA1
IL6
Link
pre
post
both
CXCR4
C5AR1
JAK2
PPIA

**Figure 3f**

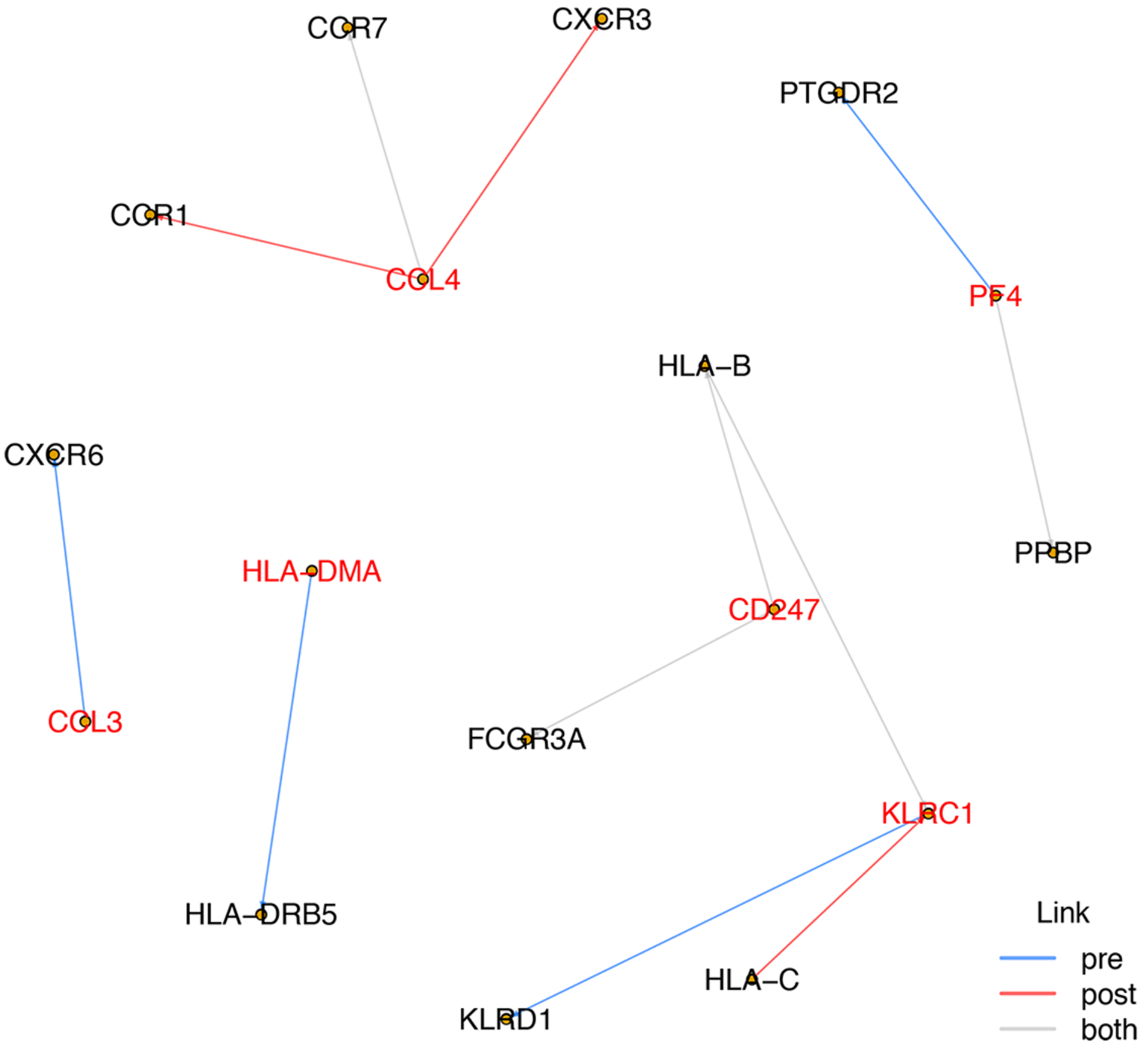
CCR7
CXCR3
PTGDR2
CCR1
CCL4
PF4
HLA−B
CXCR6
PPBP
HLA−DMA
CD247
CCL3
FCGR3A
KLRC1
HLA−DRB5
HLA−C
KLRD1
Link
pre
post
both

**Figure 3g**

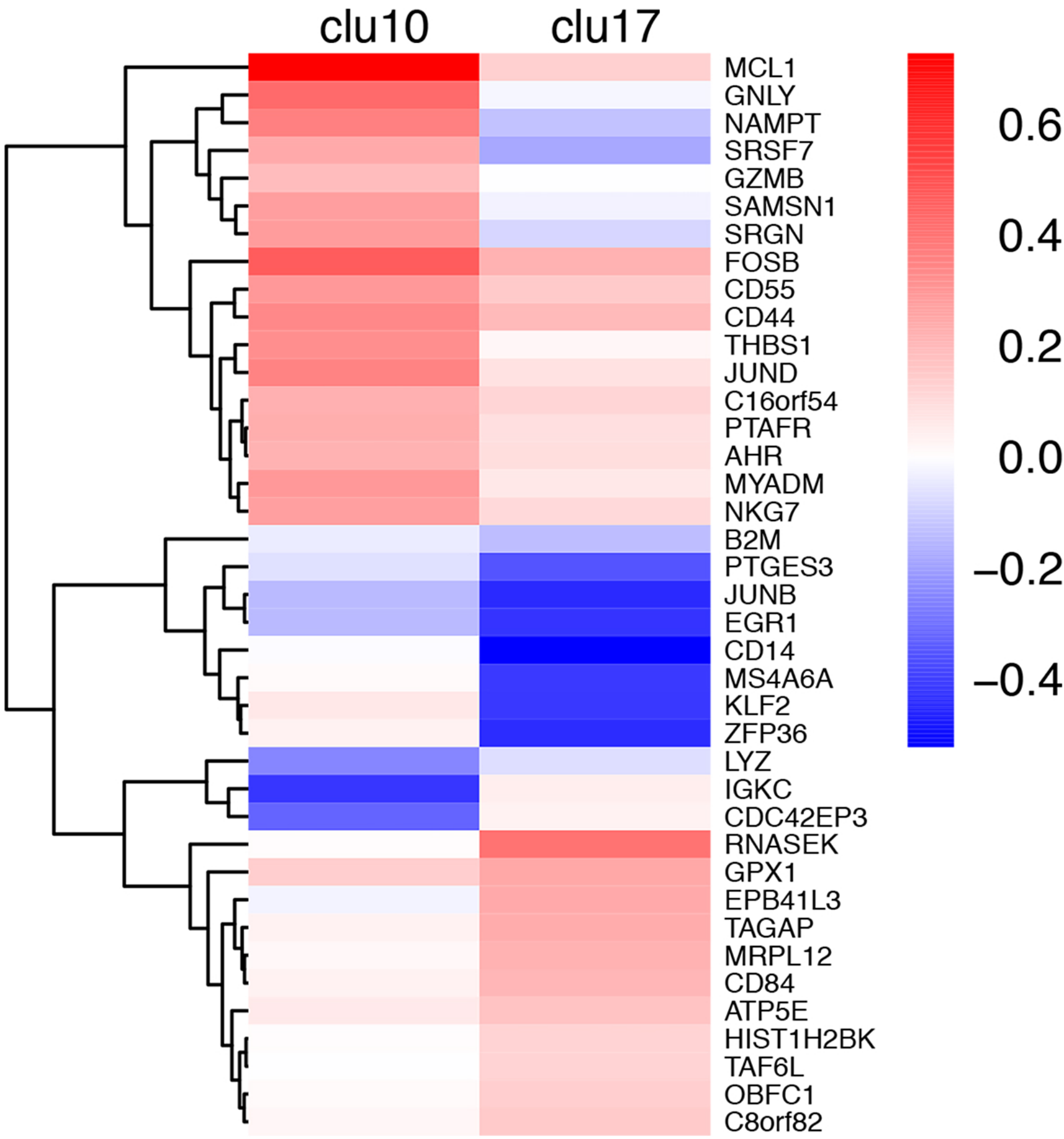
clu10
clu17
MCL1
GNLY
NAMPT
SRSF7
GZMB
SAMSN1
SRGN
FOSB
CD55
CD44
THBS1
JUND
C16orf54
PTAFR
AHR
MYADM
NKG7
B2M
PTGES3
JUNB
EGR1
CD14
MS4A6A
KLF2
ZFP36
LYZ
IGKC
CDC42EP3
RNASEK
GPX1
EPB41L3
TAGAP
MRPL12
CD84
ATP5E
HIST1H2BK
TAF6L
OBFC1
C8orf82
0.6
0.4
0.2
0.0
−0.2
−0.4

**Figure 3h**

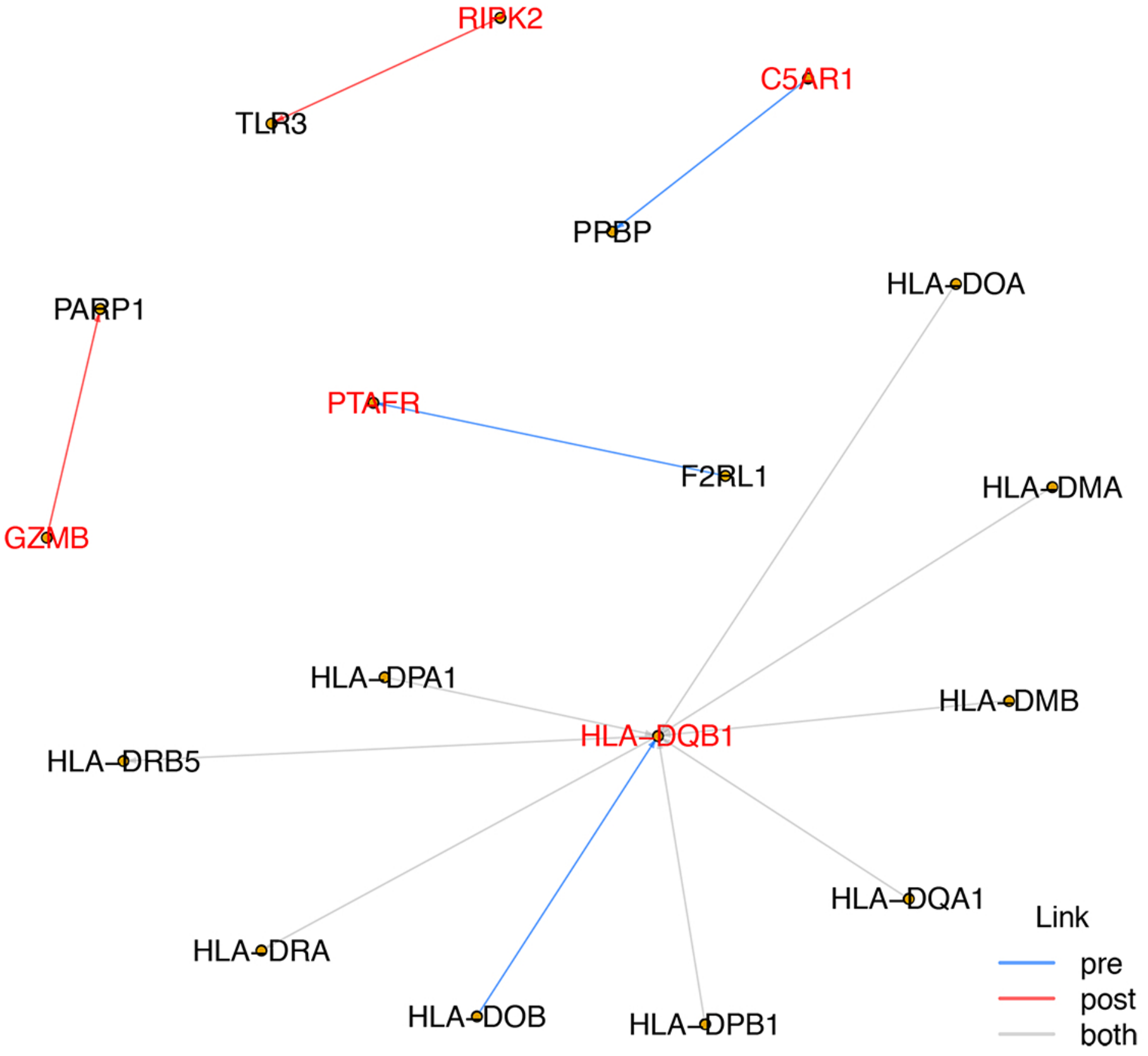
RIPK2
C5AR1
TLR3
PRBP
HLA-DOA
PARP1
PTAFR
F2RL1
HLA-DMA
GZMB
HLA-DPA1
HLA-DMB
HLA-DQB1
HLA-DRB5
HLA-DQA1
HLA-DRA
HLA-DOB
HLA-DPB1
Link
pre
post
both

**Figure 3i**

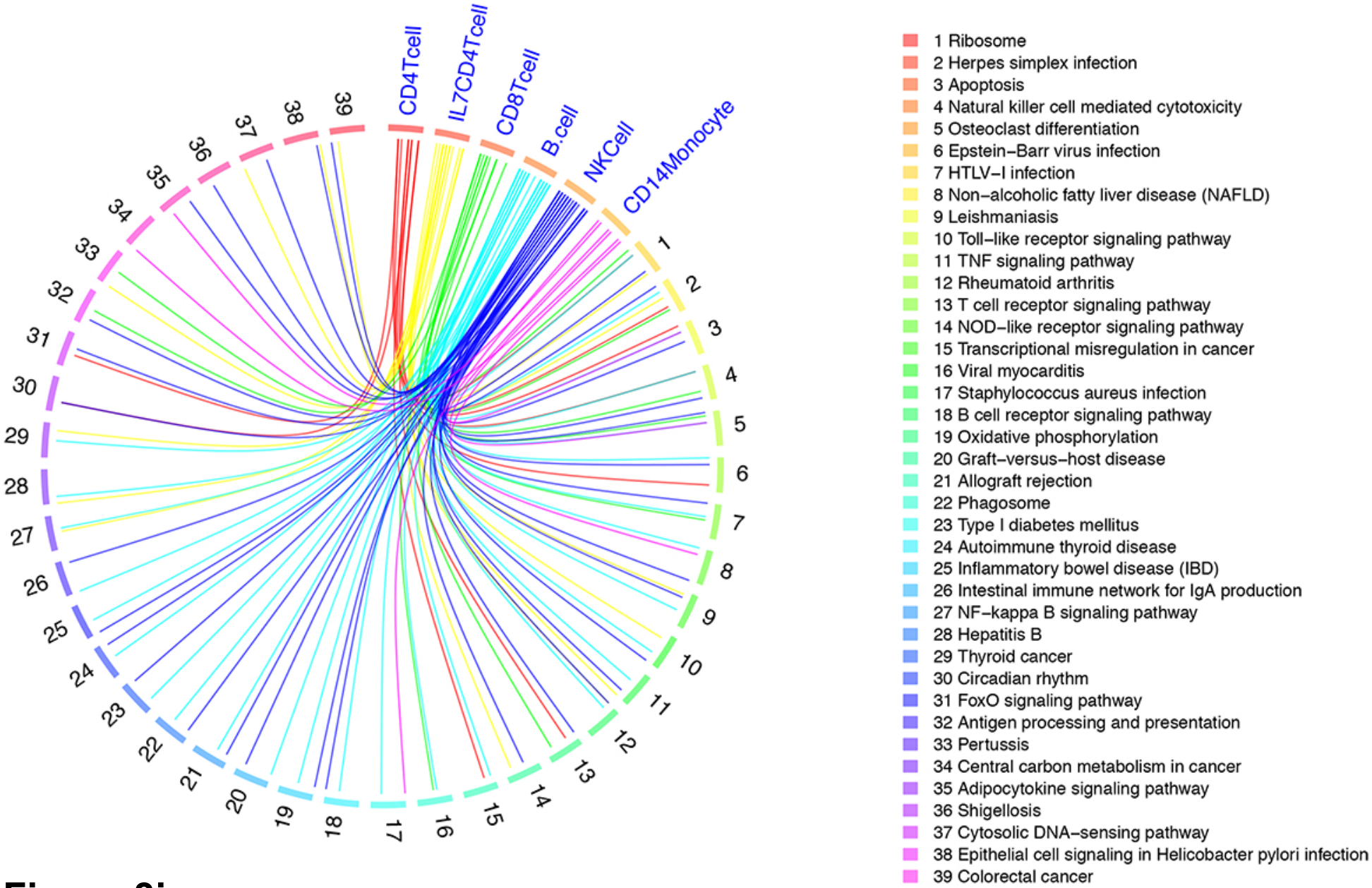
CD4Tcell
IL7CD4Tcell
CD8Tcell
B.cell
NKCell
CD14Monocyte
1 Ribosome
2 Herpes simplex infection
3 Apoptosis
4 Natural killer cell mediated cytotoxicity
5 Osteoclast differentiation
6 Epstein−Barr virus infection
7 HTLV−I infection
8 Non−alcoholic fatty liver disease (NAFLD)
9 Leishmaniasis
10 Toll−like receptor signaling pathway
11 TNF signaling pathway
12 Rheumatoid arthritis
13 T cell receptor signaling pathway
14 NOD−like receptor signaling pathway
15 Transcriptional misregulation in cancer
16 Viral myocarditis
17 Staphylococcus aureus infection
18 B cell receptor signaling pathway
19 Oxidative phosphorylation
20 Graft−versus−host disease
21 Allograft rejection
22 Phagosome
23 Type I diabetes mellitus
24 Autoimmune thyroid disease
25 Inflammatory bowel disease (IBD)
26 Intestinal immune network for IgA production
27 NF−kappa B signaling pathway
28 Hepatitis B
29 Thyroid cancer
30 Circadian rhythm
31 FoxO signaling pathway
32 Antigen processing and presentation
33 Pertussis
34 Central carbon metabolism in cancer
35 Adipocytokine signaling pathway
36 Shigellosis
37 Cytosolic DNA−sensing pathway
38 Epithelial cell signaling in Helicobacter pylori infection
39 Colorectal cancer

**Figure 3j**

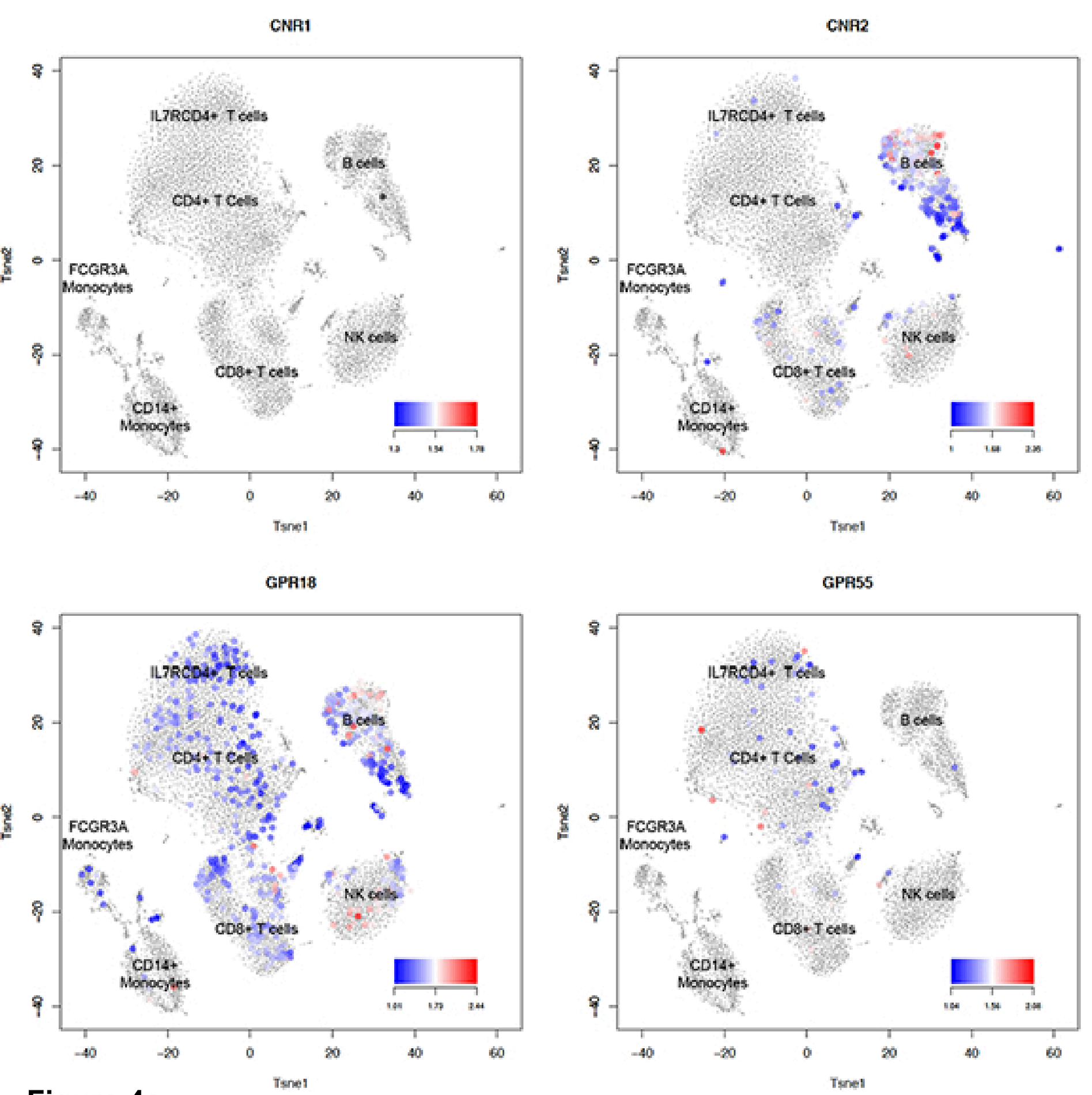
CNR1
CNR2
GPR18
GPR55
IL7RCD4+ T cells
CD4+ T Cells
B cells
FCGR3A Monocytes
NK cells
CD8+ T cells
CD14+ Monocytes
Tsne1
Tsne2

**Figure 4a**

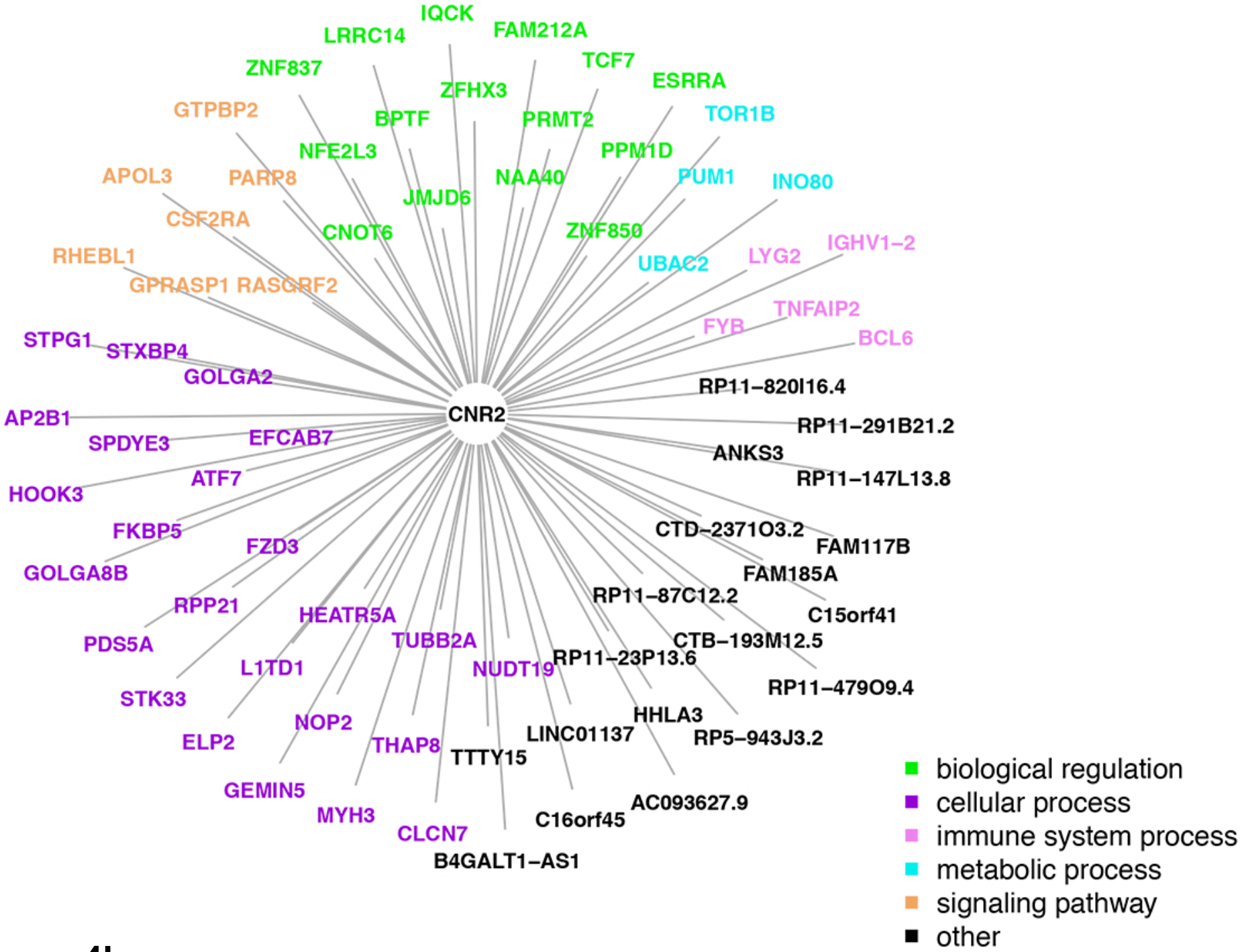
IQCK
LRRC14
FAM212A
ZNF837
TCF7
ESRRA
ZFHX3
GTPBP2
BPTF
PRMT2
TOR1B
NFE2L3
PPM1D
APOL3
PARP8
NAA40
PUM1
INO80
JMJD6
CSF2RA
CNOT6
ZNF850
IGHV1–2
RHEBL1
UBAC2
LYG2
GPRASP1
RASGRF2
TNFAIP2
FYB
STPG1
BCL6
STXBP4
GOLGA2
RP11–820I16.4
AP2B1
CNR2
RP11–291B21.2
SPDYE3
EFCAB7
ANKS3
ATF7
RP11–147L13.8
HOOK3
FKBP5
CTD–2371O3.2
FZD3
FAM117B
GOLGA8B
FAM185A
RP11–87C12.2
RPP21
HEATR5A
C15orf41
PDS5A
TUBB2A
CTB–193M12.5
L1TD1
NUDT19
RP11–23P13.6
RP11–479O9.4
STK33
HHLA3
NOP2
LINC01137
RP5–943J3.2
ELP2
THAP8
TTTY15
GEMIN5
AC093627.9
MYH3
C16orf45
CLCN7
B4GALT1–AS1
biological regulation
cellular process
immune system process
metabolic process
signaling pathway
other

**Figure 4b**